Web links to the author's journal account have been redacted from the decision letters as indicated to maintain confidentiality.

2nd Jun 20

Dear Prof Hansel,

Please allow me to apologise for the delay in sending a decision on your manuscript titled "Rapid Conversion of Isoprene Photooxidation Products in Terrestrial Plants ". It has now been seen by two reviewers, and I include their comments at the end of this message. They find your work of interest, but some important points are raised. We are interested in the possibility of publishing your study in Communications Earth & Environment, but would like to consider your responses to these concerns and assess a revised manuscript before we make a final decision on publication.

We therefore invite you to revise and resubmit your manuscript, along with a point-by-point response that takes into account the points raised. Please highlight all changes in the manuscript text file.

We are committed to providing a fair and constructive peer-review process. Please don't hesitate to contact us if you wish to discuss the revision in more detail.

Please use the following link to submit your revised manuscript, point-by-point response to the referees' comments (which should be in a separate document to any cover letter) and the completed checklist:
[link redacted]
** This url links to your confidential home page and associated information about manuscripts you may have submitted or be reviewing for us. If you wish to forward this email to co-authors, please delete the link to your homepage first **

We hope to receive your revised paper within six weeks; please let us know if you aren't able to submit it within this time so that we can discuss how best to proceed. If we don't hear from you, and the revision process takes significantly longer, we may close your file. In this event, we will still be happy to reconsider your paper at a later date, as long as nothing similar has been accepted for publication at Communications Earth & Environment or published elsewhere in the meantime.

We understand that due to the current global situation, the time required for revision may be longer than usual. We would appreciate it if you could keep us informed about an estimated timescale for resubmission, to facilitate our planning. Of course, if you are unable to estimate, we are happy to accommodate necessary extensions nevertheless.

Please do not hesitate to contact me if you have any questions or would like to discuss these revisions further. We look forward to seeing the revised manuscript and thank you for the opportunity to review your work.

Best regards,

Heike Langenberg, PhD

Chief Editor

Communications Earth and Environment

On Twitter: @CommsEarth

EDITORIAL POLICIES AND FORMATTING

We ask that you ensure your manuscript complies with our editorial policies. Please ensure that the following formatting requirements are met, and any checklist relevant to your research is completed and uploaded as a Related Manuscript file type with the revised article.

Editorial Policy: Policy requirements

Furthermore, please align your manuscript with our format requirements, which are summarized on the following checklist:
Communications Earth & Environment formatting checklist

In the event that the manuscript is accepted we will be providing further guidance on formatting but please ensure that the manuscript generally complies with our house style at this stage. The main points are as follows:

* ABSTRACT: less than 150 words and accessible. It should include the background and context of the work, the phrase 'Here we' (present/show/suggest) to indicate where the description of your own work starts, and then the methods/data, main results and conclusions of the paper.

*The text must be split into:
- INTRODUCTION (<1000 words): includes the background and rationale for the work. The final paragraph should be a brief summary of the main results and conclusions. The results of the current study should only be discussed in this final paragraph.
- RESULTS: split into subheaded sections; ensure that the subheadings are no longer than 60 characters including spaces.
- DISCUSSION: without subheadings.
- METHODS: split into subheaded sections; ensure that the subheadings are no longer than 60 characters including spaces

* SUPPLEMENTARY INFORMATION should be organised logically, with all items labelled as one of the following item types, and cited in the main article:
- Supplementary Figures, labelled and referred to as i.e. Supplementary Figure 1 throughout both the Supplementary Information and the main text
- Supplementary Tables, labelled as above
- Supplementary Notes, labelled as above
- Supplementary Discussion
- Supplementary Methods
- Supplementary References

Data: All Communications Earth & Environment manuscripts must include a section titled "Data Availability" at the end of the Methods section or main text (if no Methods). More information on this policy, and a list of examples, is available at http://www.nature.com/authors/policies/data/data-availability-statements-data-citations.pdf.
In addition, Communications Earth & Environment endorses the principles of the Enabling FAIR data project (http://www.copdess.org/enabling-fair-data-project/). We ask authors to make the data that support their conclusions available in permanent, publically accessible data repositories. (Please contact the editor if you are unable to make your data available).
In particular, the Data availability statement should include:
- Unique identifiers (such as DOIs and hyperlinks for datasets in public repositories)
- Accession codes where appropriate
- If applicable, a statement regarding data available with restrictions
- If a dataset has a Digital Object Identifier (DOI) as its unique identifier, we strongly encourage including this in the Reference list and citing the dataset in the Data Availability Statement.

DATA SOURCES: All new data associated with the paper should be placed in a persistent repository where they can be freely and enduringly accessed. We recommend submitting the data to discipline-specific, community-recognized repositories, where possible and a list of recommended repositories is provided at http://www.nature.com/sdata/policies/repositories.

If a community resource is unavailable, data can be submitted to generalist repositories such as figshare or Dryad Digital Repository. Please provide a unique identifier for the data (for example a DOI or a permanent URL) in the data availability statement, if possible. If the repository does not provide identifiers, we encourage authors to supply the search terms that will return the data. For data that have been obtained from publically available sources, please provide a URL and the specific data product name in the data availability statement. Data with a DOI should be further cited in the methods reference section.

Please refer to our data policies at http://www.nature.com/authors/policies/availability.html.

REVIEWER COMMENTS:

Reviewer #1 (Remarks to the Author):

This is a very nice study were 1,2-ISOPOOH reaction with poplar plants were shown to produce MEK and MVK in equal quantities.
the work if of great interest for the community as it proposes a process of MEK biogenic "catalysis" from 1,2-ISOPOOH. The authors propose a mechanism in which alkenal/one oxidoreductase (AOR) is responsible for that process. They then evaluate globally the amount of MEK may be formed by this process

The science is excellent and the experiments use state of the art instruments.

However some conclusions may be raised without being very solid to my point and some causality link may be missing:
1) the role of AOR in forming MEK from MVK is likely but not demonstrated per se in this study. The activity of this enzyme does not change with the dose of 1,2-ISOPOOH.
2) the location of the conversion is assumed to be the apoplasm, but this is also not stricktly demonstrated : indeed ISOPOOH is water soluble but cuticles show a microscopic layer which is wet when stomata open : it may well be that the reaction takes place on the leaves surfaces but not in the apoplasm.
3) the worldwide evaluation should be more justified ande explained: the use of the laboratory deposition velocity should be more explicited, and the fact that experiments with poplars are used to generate woldwide estimates also justified. Although the enzyme AOR is ubiquitous, its content will change with plants and its activity probably with temperature. This should be discussed.

I think that this manuscript should be published but with more discussions on the points abobe.

Reviewer #2 (Remarks to the Author):

The paper describes a new finding that ISOPOOH is quickly converted to MVK and MEK by plants and shows global emission estimate of MEK, using data including laboratory fumigation measurement, field flux measurement and global estimate model. It is worth being published by the journal after revisions described below are carefully conducted by the authors.

Fig. 2 title
Which concentration are they? inlet or outlet? except “inlet”, the other three seem to be outlet. If so, mention this.

Line 154 S. Muramoto et al.(29) did not show the relationship between stomatal opening and uptake of MVK. More accurate measurement was done by Tani et al (Environmental Science & Technology 44, 7096-7101. 2010) at low concentration of MVK and MAC. They showed a clear relationship between stomatal conductance and MVK uptake rate. They show MEK source is also plants.
Please check it and consider to cite it.

It is better to globally estimate plant uptake of MEK in addition to MEK emission, as MEK is the second abundant ketone beside acetone. MEK is absorbed by all plants including non-isoprene emitters in the world. In Fig 4, you need to add the estimate of MEK deposition onto forests. This process is also governed by stomata. If it is difficult to do this, at least mention the importance of MEK deposition onto terrestrial ecosystem by citing the papers below. These papers indicate that MEK source is also plants.
(Tani et al., 2010, Environmental Science & Technology 44, 7096-7101.; Tani et al., 2013, Atmospheric Environment 70, 300-306.; Cappellin et al., Atmospheric Chemistry and Physics 2019, 19, 3125-3135).

Line 245 How did you distinguish MEK from isomers including butanal and 2-methy propanal. They are also ubiquitous. Here you used proton-transfer reaction using H3O+?
Explain it in more detail in the MS.

Line 317 Show plant detail in material section, at least shoot dry weight and leaf area.

Line 319 You cannot extrapolate the uptake rate obtained using such infant trees to ecosystem scale. How do you link such infant tree results to adult tree one?

Line 372-389 As the description here is mostly dependent on citation, readers cannot understand the method. No supporting information is given for this part. More detailed explanation should be given in MS or SI. Especially explant how to estimate MEK emission and what deposition data of MEK including deposition velocity is basically used.

In supporting information
Line 2 In Representative poplar fumigation experiment
"In step A, we enriched the air with 7.8±1.0 ppbv of 1,2-ISOPOOH across all replicates."
The mixing ratio seems to be high if we see natural environment. It may be difficult to set it below ppbv, but authors need to explain how to extrapolate this uptake and emission results to terrestrial ecosystem.

In Experimental design
"The plants were fumigated with synthetic air (5.0 grade, Messer Austria GmbH, Gumpoldskirchen, Austria) that was mixed with CO2 (4.8 grade, Messer Austria GmbH, Gumpoldskirchen, Austria)"
The air and pure CO2 are not perfectly pure, possibly including other compounds that may interfere the measurement. Authors need to check the contamination level of the air before doing experiment using GCMS.

In "Representative poplar fumigation experiment"
How did you avoid water vapor condensation onto inner surface of the enclosure bag?

In "Infrared gas analyzer (IRGA)"
What is the flow rate to IRGA? Especially water vapor is also sticky and needs to relatively high flow rate.

Equation (4) and (5) The equations are not correct in this case. The outlet air is more humidified by plant transpiration and the flow rate F is not same between the inlet and outlet, usually 1-2% higher in the outlet. You need to add humidity-correction term in the equation. The paper shown below is source of the equation and refer it please.
von Caemmerer, S.; Farquhar, G. D. Some relationships between the biochemistry of photosynthesis and the gas exchange o leaves. Planta 1981, 153 (4), 376–387.

Rapid conversion of isoprene photooxidation products in terrestrial plants

Authors: Eva Canaval[1], Dylan B. Millet[2], Ina Zimmer[3], Tetyana Nosenko[3], Elisabeth Georgii[4], Eva Maria Partoll[1], Lukas Fischer[1], Hariprasad D. Alwe[2], Werner Jud[3], Markku Kulmala[5], Thomas Karl[6], Jörg-Peter Schnitzler[3], Armin Hansel[1*]

Affiliations:

[1]Department of Ion Physics and Applied Physics, University of Innsbruck, Innsbruck, Austria.

[2]Departement of Soil, Water and Climate, University of Minnesota, 439 Borlaug Hall, St. Paul MN, USA

[3]Helmholtz Zentrum München, Institute of Biochemical Plant Pathology, Research Unit Environmental Simulation, Neuherberg, Germany.

[4]Helmholtz Zentrum München, Institute of Biochemical Plant Pathology, Neuherberg, Germany

[5]Institute for Atmospheric and Earth System Research (INAR) / Physics, University of Helsinki, Helsinki 00014, Finland.

[6]Institute of Atmospheric and Cryospheric Sciences, University of Innsbruck, Innsbruck, Austria.

*Correspondence to: armin.hansel@uibk.ac.at

Isoprene is the dominant non-methane hydrocarbon emitted from the biosphere into the atmosphere, where it is preferentially oxidized to isoprene-hydroxy-hydroperoxides (ISOPOOH) at low NO_x or to methyl vinyl ketone (MVK) and methacrolein (MACR) at high NO_x. Here we show that 1,2-ISOPOOH deposits rapidly into poplar leaves where it undergoes conversion first to cytotoxic MVK and then enzymatically to less toxic methyl ethyl ketone (MEK), which is emitted into the atmosphere. We analyzed *in situ* alkenal/one oxidoreductase (AOR) activity in leaf extracts from poplar plants fumigated with either 1,2-ISOPOOH or MVK and found that this enzyme was constitutively present in all leaf samples. This detoxification process has global significance because AOR enzymes are ubiquitously present in terrestrial plants. Global chemistry-transport model simulations imply a re-emission of MEK from vegetation of 6.1 Tg yr^{-1}, making this the single largest MEK source and recycling 1.5 % of the original isoprene flux. Eddy covariant flux measurements of isoprene and MEK over forests confirm that these MEK emissions reach 1-2 % those of isoprene. Our results suggest that detoxification processes in plants provides one of the most important OVOC sources in the atmosphere.

Biogenic volatile organic compounds (BVOC) are thought to account for 90% of the total VOC emission into the Earth's atmosphere (*1*). Isoprene (C_5H_8) is the dominant BVOC with an estimated annual flux of 350-800 Tg yr^{-1} (*2*). Despite this large flux (mainly from broadleaf tree species) the question of why plants emit isoprene is still unresolved (*3*). Recent hypotheses suggest that isoprene acts as a signaling molecule that, by altering gene expressions, strengthens plant defense mechanisms against oxidative stress (*4*). Once in the atmosphere isoprene reacts rapidly with OH radicals, which account for 90% of its total sink (*5*). Under typical daytime conditions isoprene is thus converted to oxidized VOC (OVOCs) within 1-2 hours (*6*). OH preferentially add to the terminal carbons of isoprene, forming allyl radicals that in collisions with oxygen react to form HO-$C_5H_8O_2$ (ISOPOO) radicals. Subsequent oxidative steps depend critically on the ambient abundance of NO_x (NO + NO_2). At elevated NO_x, ISOPOO predominantly reacts with NO to form methyl vinyl ketone (MVK, yield 30-45%), methacrolein (MACR, yield 20-30%), and isoprene hydroxy nitrate (IHN, yield 13%) plus formaldehyde (HCHO) as the major products (*7*). Under low NO_x conditions the main product of ISOPOO reacting with HO_2 is isoprene hydroxy hydroperoxide (ISOPOOH), with the 1,2-ISOPOOH isomer formed in highest yield (*5*). Recently, Nguyen et al. (*8*) applied the eddy covariance (EC) technique to quantify the rapid dry deposition of ISOPOOH and other oxidized BVOC to a temperate forest. They determined a daytime mean deposition velocity (v_d) for ISOPOOH + IEPOX of 2.5 cm s^{-1} (IEPOX is an isomeric photooxidation product of ISOPOOH + OH). ISOPOOH+IEPOX deposition velocities (v_d) were then compared with a resistance model described elsewhere (*9*, *10*) to evaluate whether ISOPOOH+IEPOX is primarily lost to the leaf surface or taken up by the plants through their stomata. The calculated Henry's law constant of ISOPOOH+IEPOX suggests a very small residual resistance favoring efficient uptake to any

liquid surfaces (*8*). However, the v_d for ISOPOOH+IEPOX measured by Nguyen et al. (*8*) was too close to both the upper limit for stomata-controlled resistance and the upper limit for deposition without surface resistance to tell which mechanism is dominant. Thus, while direct EC flux measurements quantify the deposition of chemical species to the canopy, the fate of species at the leaf level – and thus any associated ecological impact – cannot be evaluated in this way. In the present study, we combine uptake rates and deposition velocities for 1,2-ISOPOOH and MVK obtained in laboratory experiments on gray poplars (*Populus* x *canescens*) with field observations using the EC technique in natural forest settings. Furthermore, we quantify the gene expression and enzyme activity of the detoxifying NADPH-dependent enzyme alkenal/one oxidoreductase (AOR) in poplar leaves and demonstrate the worldwide dissemination of AOR genes across terrestrial plants. Finally, we apply chemistry-transport modeling to assess atmospheric implications of our findings (see Methods for details). This enables the first leaf-to-global scale description of biosphere-atmosphere exchange for major isoprene photooxidation products, as summarized in Fig. 1.

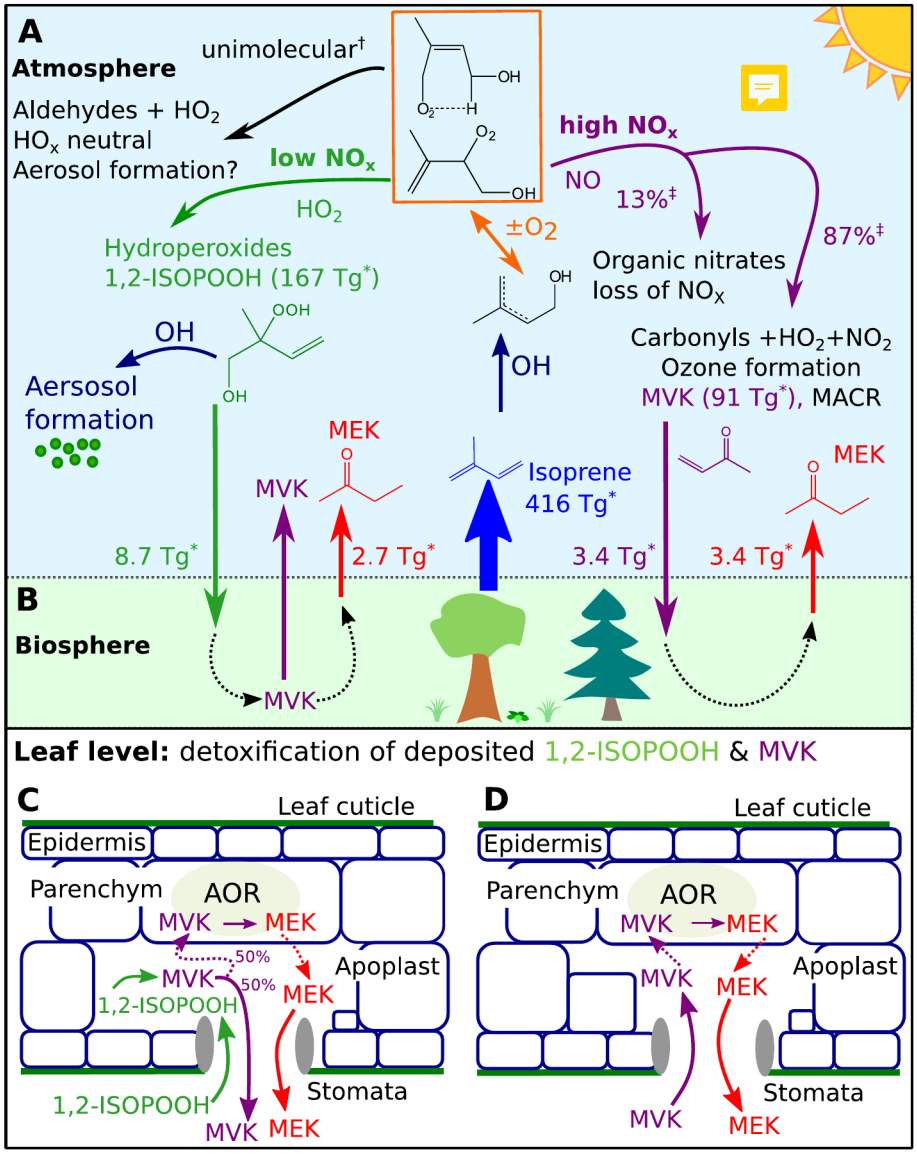

Fig. 1 Organic carbon exchange of major isoprene photooxidation products between the biosphere (B) and the atmosphere (A) on a global scale. Under low NO_x conditions 1,2-ISOPOOH is preferentially formed, producing epoxides that then react with OH and contribute to aerosol formation (*11*). At high NO_x the production of carbonyls such as MVK supports ozone formation (*5*). Dry-deposited 1,2-ISOPOOH and MVK is instantaneously detoxified within the plant leaf (C) via the enzyme alkenal/one oxidoreductase (AOR). EC measurements in natural forest settings confirm our modified GEOS-Chem model results (indicated with *) that approximately 6.1 Tg MEK (corresponding to 1.5% of the isoprene source) is emitted into the

atmosphere in this way. This is the single largest known MEK source on a global scale. † Values from ref. (*12*). ‡ Values from ref. (*7*).

Results from enclosure experiments

In a laboratory study we investigated the fate of isoprene oxidation products when exposed to poplar leaves (Fig. 2, S1-4). The experimental setup is illustrated in Figure S1. Gray poplar plants were placed in an enclosure system and fumigated with synthetic air containing ~450 ppm CO_2 and ~8 ppbv 1,2-ISOPOOH. Before starting the plant fumigation experiments, we fumigated the empty cuvette with 1,2-ISOPOOH to condition the inner surfaces consisting of Teflon coated glass. Subsequently, the 1,2-ISOPOOH loss to the surface of the empty enclosure was measured for each individual experiment. The OVOC composition of the inlet and outlet air of the plant enclosure was analyzed with a selective reagent ion time-of- flight mass spectrometer (SRI-TOF-MS). Details of the measurement method, SRI-TOF-MS instrument calibration, and plant material can be found in Methods and SI.

The deposition velocity $v_{d,i}$ (cm s^{-1}) is commonly used to describe trace gas deposition of a substance i to vegetation from the atmosphere (*13*) and is defined as the ratio between the flux Φ_i (representing the amount of compound i deposited to a unit surface area per unit time) and the local concentration c_i.

$$v_{d,i} = -\Phi_i / c_i \quad (1)$$

Deposition fluxes Φ_i to the plant surfaces inside the enclosure system were calculated from the difference in trace gas mixing ratios between the inlet ($c_{i,in}$) and outlet ($c_{i,out}$) taking into account the single-sided leaf area (LA) of the enclosed plant and the gas flow (see SI). In this way we calculated an average 1,2-ISOPOOH deposition velocity of v_d= 0.10 ± 0.03 cm s^{-1} under

dark conditions (Fig. 2). The observed daytime value with open stomata (Fig. S5) is 0.78 ± 0.15 cm s^{-1}, close to the 24-h average simulated v_d of 0.76 cm s^{-1} from Nguyen et al. (*8*). Almost all deposited 1,2-ISOPOOH thus enters through open stomata into the plant's inner space, where it will dissolve on wetted surfaces due to its large effective solubility ($H^* = 1.7x10^6$ M atm^{-1}). We further determine from these experiments that 50±15% of stomatal-deposited 1,2-ISOPOOH is released as the volatile carbonyl MVK ($H^* = 44$ M atm^{-1}) while the other 50% is converted to MEK ($H^* = 21$ M atm^{-1}), which is likewise released back into the atmosphere.

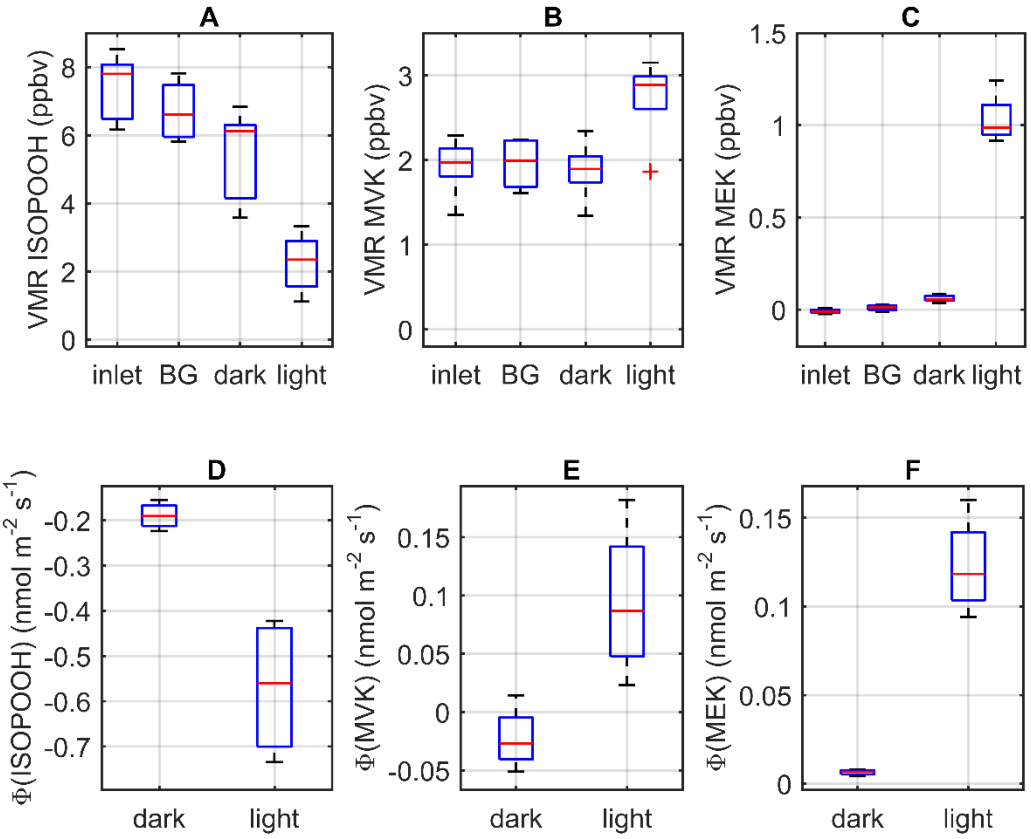

Fig. 2: Box plots of volume mixing ratios (VMR) (A-C) and deposition/emission fluxes (Φ) (D-F) for 1,2-ISOPOOH, MVK and MEK, respectively. OVOCs were analyzed at the enclosure inlet and subsequently at the enclosure outlet during fumigation of the empty enclosure (BG) and of the darkened/illuminated gray poplar trees. For each box, the red line indicates the median, bars show the minimum/maximum, and the blue box indicates the 25th and 75th percentiles of the sample data (N=5).

Organic hydroperoxides are inherently unstable species. Homolytic cleavage of the weak peroxy bond (O-OH) is a common decomposition mechanism, and can be catalyzed by metals (*14*). Recently, we have shown that 1,2-ISOPOOH is efficiently converted to MVK and HCHO on clean stainless steel surfaces (*15*, *16*). We find here from separate laboratory experiments (Fig. S6) that a range of different metals catalyze the conversion of 1,2-ISOPOOH to MVK even at room temperature. Chevallier et al. 2004 (*17*) studied "Fenton-like" reactions of methylhydroperoxides with Fe^{2+} in aqueous solutions. They identified $Fe^{2+} + ROOH \rightarrow Fe^{3+} + RO + OH$ as the dominant first reaction step. The alkoxy (RO) radicals further rearrange in water solution, and react with dissolved oxygen to form peroxy radicals which decompose, leading to the formation of aldehydes and other products. Assuming that the same reaction mechanism occurs when ISOPOOH dissolves in the liquid phase of the apoplast, low-valence transition metals present in plant cell walls and also dissolved in the apoplast (*18*) could catalyze via Fenton-type reactions the conversion of 1,2-ISOPOOH to MVK + HCHO + HO_2 in plant leaves. Since MVK (in contrast to formaldehyde) has relatively low solubility, it would then be released into the atmosphere through open stomata as its concentration builds up in the liquid phase of the apoplast. In biological systems peroxide functional groups (ROOH) serve as reactive oxygen intermediates that cause oxidative damage and cell death (*19*). For example, Polle and Junkermann (*20*) found hydroxymethyl hydroperoxide (HMHP) to inhibit peroxidase activity in plant apoplast. Plants exposed to harmful compounds in this way typically release stress-induced volatiles such as methyl salicylate (MeSA). MeSA is an airborne cue inducing pathogen resistance within and between plants (*21*), while also enhancing indirect plant defenses against herbivores by attracting their natural enemies (*22*). Furthermore, unstressed poplar varieties in general are weak sesquiterpene (SQT) emitters (*23*), but SQT emissions are known to increase

under various type of abiotic and biotic stresses (*24*, *25*). Here we observe a significant increase in emissions of both MeSA and SQT during 1,2-ISOPOOH fumigation (Fig. S7), but only under daylight conditions when stomata are open. Our laboratory experiments therefore indicate that stomatal uptake of 1,2-ISOPOOH causes severe stress to poplar plants and triggers self-defense mechanisms to mitigate oxidative damage. The results also indicate that upon deposition to plants, 1,2-ISOPOOH is converted as a first step to MVK. The exact reaction mechanism of this first step is not known. However, we speculate that the Fenton-type reactions discussed above involving transition metals present in plant cell walls and dissolved in the apoplast (18) catalyze the conversion of 1,2-ISOPOOH to MVK. As an α,β-unsaturated carbonyl and reactive electrophilic species, MVK itself is toxic to plant tissue due to its high reactivity and ability to form Michael adducts with the thiol and amino groups of biomolecules (*26*)(*27*). Previous MVK and MACR deposition experiments using poplars and tomatoes have found both compounds to be immediately lost upon entry through open stomata (*28*)(*29*). Further, Cappellin et al. (*30*)(*31*) found that red oak (a strong isoprene emitter) converts MVK to MEK. Here we find based on additional MVK fumigation experiments with gray poplar plants (Fig. S4) that upon stomatal opening MVK fumigation leads to a significant increase in stress-related MeSA and SQT emissions (Fig. S7). Furthermore, the MVK detoxification mechanism is highly efficient: all (100±5%) deposited MVK is released as MEK into the atmosphere (Fig. S4). Average deposition velocities for MVK of v_d = 0.014 ± 0.0014 cm s^{-1} and 0.22 ± 0.02 cm s^{-1} during dark and light conditions, respectively, are derived, demonstrating the importance of stomatal fluxes for this process. Poplar fumigation experiments with the 4,3-ISOPOOH isomer did not result in any MEK production. This finding is expected and supports above proposed mechanism because 4,3-ISOPOOH is converted on metal surfaces to methacrolein (MACR) rather than MVK (*15*, *16*).

Enzymatic reactions within plant tissues

Several studies have shown that enzymatic reduction of α,β-unsaturated ketones takes place in plant suspension cells and cytosolic fractions of yeast (*32*, *33*). In particular, Yamauchi et al. (*34*) identified an NADPH-dependent acrolein-reducing enzyme in cucumber leaves that catalyzes an alkenal/one oxidoreductase (AOR) reaction of the α,β-unsaturated bond. We find in our experiments a constitutively present *in vitro* AOR (EC 1.3.1.74) activity in leaf extracts, to which we attribute the *in planta* conversion of MVK to MEK. This biochemical capability to reduce MVK to MEK is globally present in terrestrial plants, as a phylogenetic survey of genes coding for NADPH-dependent alkenal/on-oxidoreductases (AOR) demonstrates (Fig. 3, S8). One gene encoding AOR is localized in the chloroplast (AORchl), and two more are located in the cytosol (AORcyt-I and AORcyt-II; Fig. 3B and S8). The distribution of AORchl and AORcyt in plants is independent of isoprene and monoterpene emissions (Fig. 3A): AOR genes are ubiquitous in all land plants including mosses, clubmosses, gymnosperm and flowering plants (Fig. S8). Our gene expression analyses for gray poplar show that AORchl is predominantly expressed in leaf tissue, while AORcyt-II is expressed in the stem (phloem and xylem) (Figure 3B). Under normal environmental conditions (*35*) the total gene expression rates of AORchl are more than six times those of AORcyt-II. We analyzed *in situ* AOR activity in leaf extracts from poplar plants fumigated with either 1,2-ISOPOOH or MVK (Fig. S9). AOR activity was present in all leaf samples (and unchanged during the short period of exposure to 1,2-ISOPOOH or MVK). The phylogenetic analysis and the measurements of AOR activity in our model tree system imply that green biomass across the globe is able to convert MVK to MEK.

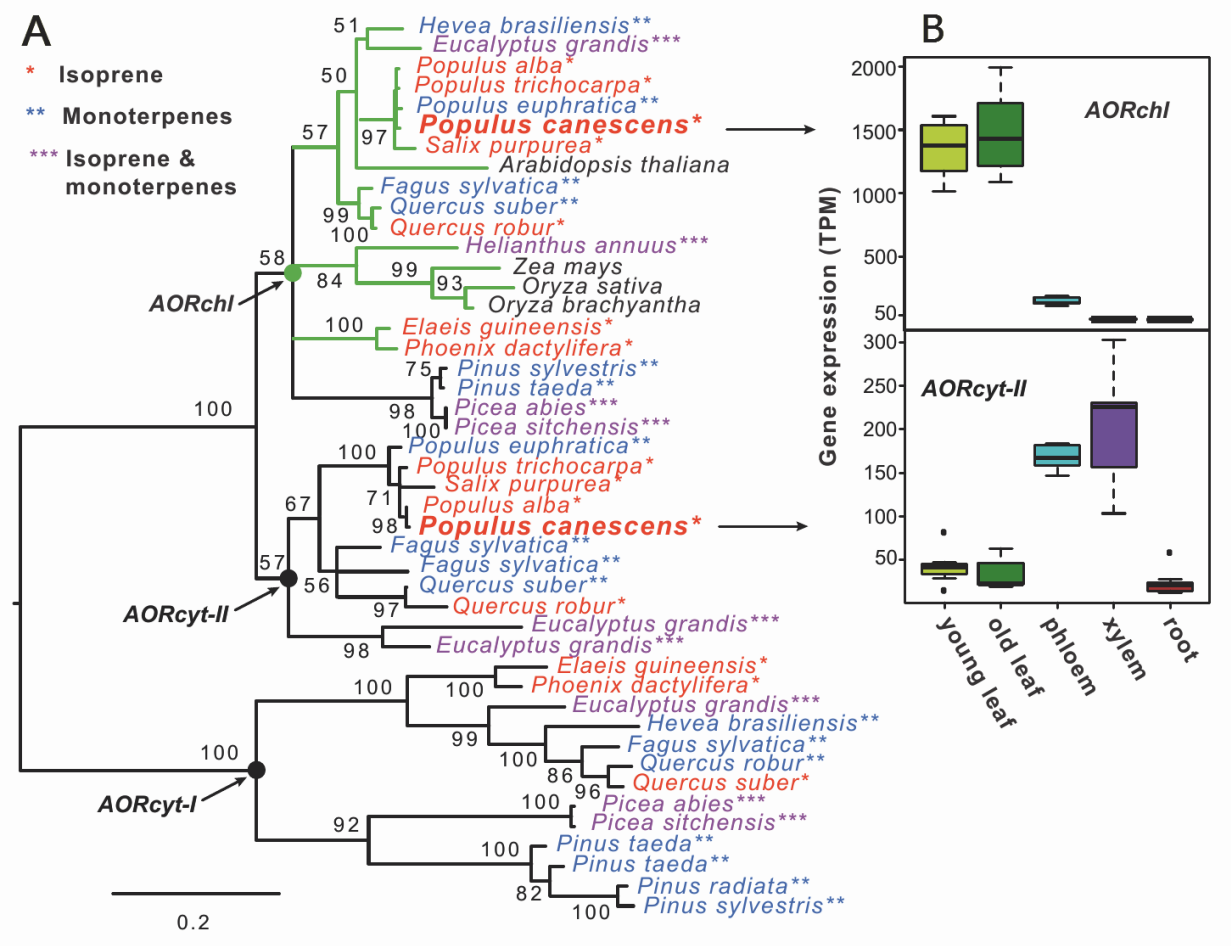

188

189 **Fig. 3:** Distribution of genes encoding AOR proteins. The Maximum likelihood (ML)
190 phylogenetic tree (A) shows the occurrence of *AORchl*, *AORcyt-I* and *AORcyt-II* genes in
191 dominant plant species. Asterisks and coloring of the branch labels indicate species emitting
192 predominantly isoprene, monoterpenes, or both. Numbers at tree branches indicate node
193 bootstrap support. Green branch coloring indicates the presence of plastid-targeting peptides
194 (TP) in the corresponding AOR sequences. Basal nodes of the *AORchl*, *AORcyt-I* and *AORcyt-II*
195 ortholog clusters are labeled with solid circles. The scale bar below the tree shows branch length.
196 Box plots (B) show tissue-specific expression of *AORchl* and *AORcyt-II* genes in gray poplar
197 (*Populus* x *canescens*).

198 **Impact on regional and global budgets of OVOCs**

199 We performed global simulations using the GEOS-Chem chemical transport model (CTM)

200 (v12.1.1, doi:10.5281/zenodo.2249246) to assess how dry deposition of 1,2-ISOPOOH and

MVK (as the main isoprene oxidation products) impact the atmospheric MEK budget (see Methods and SI for model details). A global emission of 416 Tg isoprene is simulated by the model for 2017, leading to the photochemical production of 91.3 Tg MVK and 167 Tg 1,2-ISOPOOH (Fig. 4). By default, GEOS-Chem uses a modified resistance-based approach from Wesely (*9*) to calculate dry deposition velocities. The performance of this approach depends on knowledge about atmospheric stability, surface conditions, and the solubility and reactivity factors f_0 for compounds of interest. The stomatal fraction of 1,2-ISOPOOH dry deposition thus simulated by the model generally ranges from <5% to 30% over land (Fig. S10), which does not agree with our findings here (v_d = 0.78 cm s^{-1} during daytime versus only 0.10 cm s^{-1} in the dark). We therefore question how accurately the default model scheme is able to separate stomatal versus non-stomatal deposition for OVOCs. Instead, we prescribe the modeled 1,2-ISOPOOH and MVK deposition velocities over land based on the results from our laboratory measurements (over oceans the default Wesely scheme is used). Since the laboratory chambers were well-mixed, this corresponds to an assumption that canopy uptake for these compounds is controlled by surface and molecular diffusion (rather than aerodynamic) resistance, an assumption strongly supported by prior work (*8*). Figure 4 shows the resulting simulated deposition of MVK (3.4 Tg) and 1,2-ISOPOOH (8.7 Tg). Assuming based on our measurements that 100% of dry deposited MVK and 50% of dry deposited 1,2-ISOPOOH undergoes conversion to MEK, the model yields a global MEK flux of 6.1 Tg (1.5% of isoprene emissions, Fig. S11), making this mechanism the largest known MEK source to the atmosphere (*36*).

For comparison, we performed a GEOS-Chem base-case run (Fig. S12) in which the default Wesely scheme was used to simulate 1,2-ISOPOOH and MVK dry deposition. Assuming that only the stomatal component of deposition leads to MEK then yields a global source of 3 Tg. We

224 view this as a lower limit given the apparent underestimate of OVOC stomatal uptake in the
225 default model. On the other hand, assuming that all dry deposited MVK and 50% of all dry
226 deposited 1,2-ISOPOOH undergoes conversion results in an MEK source of 14 Tg (upper limit).
227

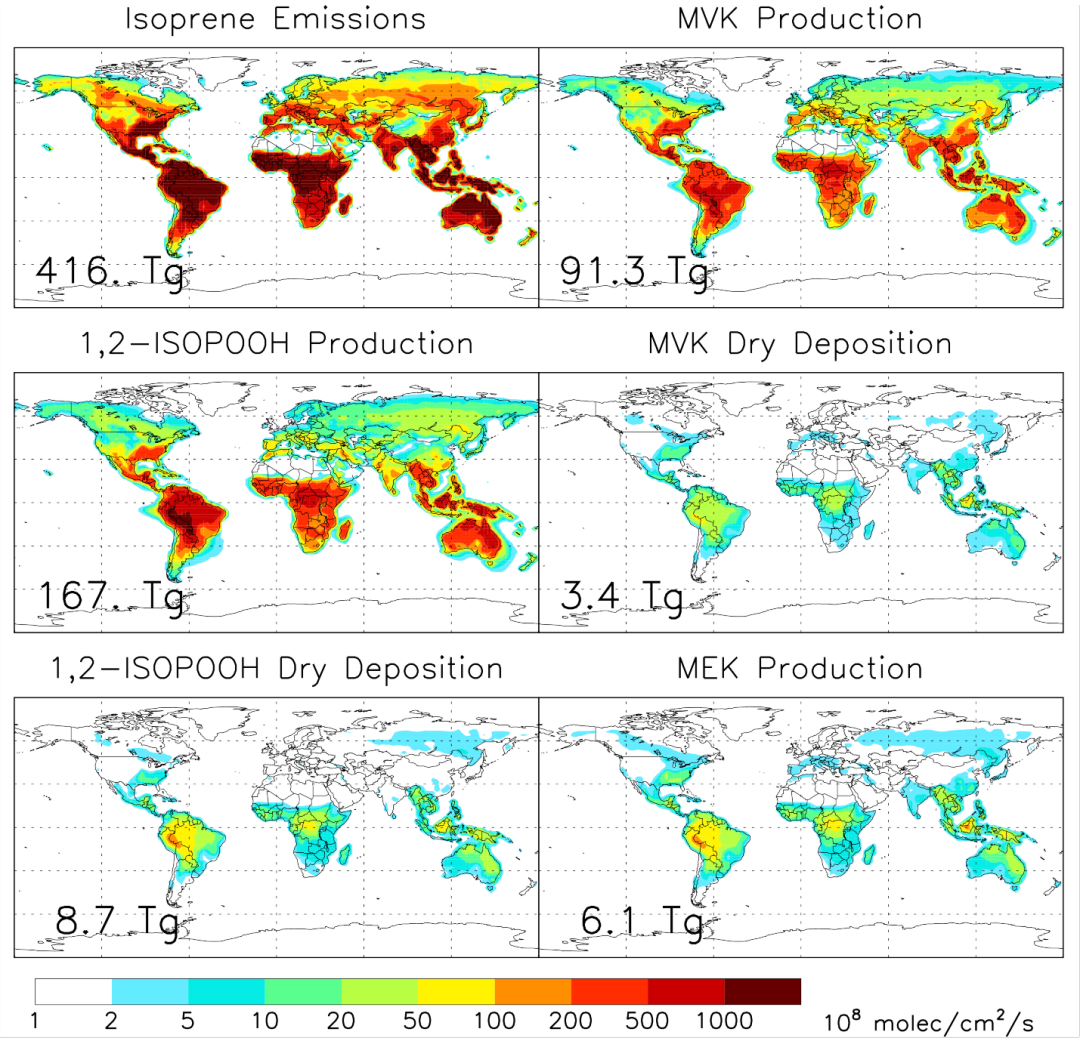

Fig. 4. Global isoprene emissions along with the production and deposition of key oxidation products (1,2-ISOPOOH, MVK) as simulated by the GEOS-Chem CTM for 2017 (see SI for model details). Reconciling the model deposition velocities using our experimentally-obtained v_d, and assuming that 100% of dry deposited MVK and 50% of dry deposited 1,2-ISOPOOH undergoes conversion in plants, reveals a global MEK source of 6.1 Tg (and recycling 1.5% of the isoprene flux).

Eddy covariant VOC flux measurements

To evaluate these findings, we performed eddy covariant (EC) flux measurements of isoprene and MEK at two sites. The first is the SMEAR II station in Hyytiälä (Finland) (Fig. S13), which is surrounded by low isoprene-emitting plants (mainly Scots pine *Pinus sylvestris*) with an

239 average daytime isoprene flux of 1 nmol m^2 s^{-1} in spring. Details of the eddy covariant VOC flux
240 measurements can be found in Methods and SI. The second EC flux measurements were
241 performed at PROPHET (US) (Fig. S14), which is a high isoprene emission site in a mixed
242 deciduous/coniferous forest. Typical daytime isoprene flux values at PROPHET reach ~10 nmol
243 m^2 s^{-1} (Fig. S14). Flux data for isoprene and MEK were obtained using the eddy covariance (EC)
244 method, correlating fast mixing ratio changes (~10 Hz) with vertical wind velocities. The high
245 sensitivity achieved by the PTR3-TOF for MEK (>12 000 cps/ppbv) enabled the first accurate
246 measurement of these fluctuations at the low isoprene-emission site. In general, the recent
247 development of very sensitive, fast and quantitative mass spectrometry-based detectors such as
248 PTR-QiTOF and PTR3-TOF (*37*) was essential for EC measurements of MEK. We find that
249 MEK emissions are 1.8 % and 0.9 % those of isoprene, at these sites respectively. This is in
250 excellent agreement with the model best-estimate (1.5%; see also Fig. S11) and supports the
251 global importance of this mechanism for plant oxidative protection and for the biogenic MEK
252 atmospheric source.

253 **Atmospheric implications**

254 Ketones are an important class of OVOC with sufficiently long atmospheric lifetimes to be
255 transported to the upper troposphere. MEK, like acetone, photolyzes in the near UV region; as a
256 result, these ketones provide an important source of HO_x ($OH + HO_2$) radicals in the dry upper
257 troposphere (*38*)(*39*). Degradation of MEK in the lower atmosphere generates toxic and photo-
258 active compounds such as acetaldehyde, a peroxyacetylnitrate (PAN) precursor, and
259 formaldehyde (*40*). Global sources of MEK, the second most abundant atmospheric ketone, are
260 still not fully understood. Singh et al. (*36*) presented a first assessment of MEK sources and sinks
261 based on aircraft measurements over the Pacific Ocean. Based on their derived MEK

atmospheric burden and an assumed 7-day lifetime due to reaction with OH and photolysis, they inferred a total global source of 11 Tg yr^{-1}. They further estimated MEK sources of 1-3 Tg yr^{-1} each from hydrocarbon oxidation and biomass burning, and of 0-1 Tg yr^{-1} from oceanic emissions. The latter estimate is supported by more recent analysis by Brewer et al. (*41*). A residual unexplained source of 7 Tg yr^{-1} was then attributed by Singh et al. (*36*) to direct biogenic emissions. Our work combining dedicated laboratory, field, and model analyses derives a global biogenic MEK source of 6.1 (3-14) Tg yr^{-1}, and provides for the first time a mechanistic foundation for understanding and modeling these emissions.

Conclusion

Plants possess the ability to absorb OVOCs from the atmosphere and actively convert toxic chemicals to less toxic species, which can then be re-emitted into the atmosphere. Here we show that following stomatal uptake the toxic isoprene oxidation products 1,2-ISOPOOH and MVK are converted and re-emitted as MEK. The genes coding for the responsible enzyme alkenal/an oxidoreductase (AOR) are ubiquitously distributed in the plant kingdom. For MEK this process leads to an atmospheric input of about 6.1 Tg, the single largest known term in the global MEK budget and re-emitting 1.5% of the original isoprene emissions. Our findings thus support and provide a mechanistic underpinning to understand the biogenic emissions inferred by Singh et al. (*36*), and implicate detoxification as the most important source process in the global MEK budget. These findings suggest a significant modification of OVOCs at the biosphere-atmosphere interface. Traditional dry deposition schemes that are widely used in atmospheric chemistry models do not capture this process, and new mechanistic approaches should be developed to capture the complex behavior of bi-directional exchange at the biosphere-atmosphere interface.

Methods

The *selective reagent ion time-of- flight mass spectrometer (SRI-TOF-MS)* is a custom-built instrument that represents an advanced version of the PTR-TOF-MS system described by Graus et al. (*42*), and features the capability to switch between different reagent ions within seconds. Additionally, we replaced the standard metal drift rings of the reaction chamber with chemically inert conductive PEEK rings. This feature and the high flow rate through the reaction chamber (~800 ml min^{-1} instead of 10-30 ml min^{-1} in standard PTR-MS instruments) were essential for minimizing metal-catalyzed decomposition of 1,2-ISOPOOH as observed in standard PTR-MS instruments (*15*). The OVOC composition of the inlet and outlet air of the plant enclosure system was sequentially analyzed by SRI-TOF-MS operated with ammonia (NH_4^+) and occasionally with nitronium (NO^+) or hydronium (H_3O^+) reagent cations. The SRI-TOF-MS was operated at a constant temperature (35°C) and pressure (2.3 mbar) in the drift tube. Different drift voltages of 250, 300 and 500 V resulting in E/N values of 45 Td (NH_4^+-mode), 54 Td (NO^+-mode) and 90 Td (H_3O^+-mode), respectively, were used (E is the electric field strength, while N is the number gas density; 1Td = 10^{-17} Vcm^2). Raw data analysis was performed with the PTR-TOF-Data Analyzer (*43*) and the data processing routine described in Breitenlechner et al. (*37*). For details about chemical ionization mechanism and calibration of the SRI-TOF-MS see the Supplementary Information.

The recently developed *PTR3-TOF* instrument (*37*) uses a discharge ion source coupled to a contact-free inlet system running at high sample gas flow rates through the novel reaction chamber at 80 mbar. The PTR3 front portion is coupled to a TOF from TOFWERK mass analyzer. The instrument has sensitivities of up to 20 000 cps per ppbv and a mass resolution of

approximately 8 000 m/Δm. VOCs were ionized via reactions with $H_3O^+(H_2O)_n$ primary ions. Flux data for isoprene and MEK were obtained using the eddy covariance (EC) method, correlating fast mixing ratio changes (~10 Hz) with vertical wind velocities. The high sensitivity achieved by the PTR3-TOF for MEK (>12 000 cps/ppbv) enables more accurate measurement of these fluctuations than was previously possible. Calibration details are described in the Supplementary Information.

In the present study we used 4-month old gray poplars (*Populus* x *canescens* INRA clone 7171-B4; syn. *P. tremula* x *P. alba* (Aiton.) Smith). Gray poplar shoots had been amplified by micropropagation on half-concentrated MS medium and further cultivated at the Helmholtz Zentrum München to an age of three months as described elsewhere (*44*). Before being used in the experiments, the poplar plants were grown in a greenhouse at the Institute of Microbiology of the University of Innsbruck for 1 to 4 weeks under natural light conditions. One day prior to the experiment, the plants were transferred to the laboratory to adapt to the light conditions (12-hour photoperiod with an approximate PAR of 400 µmol photons m^{-2} s^{-1}). All plants were well watered and showed no visible illness symptoms.

To determine apparent *in vitro* AOR activities in poplar leaf protein extracts, we deep-froze three mature leaves (leaf # 9-11, below the apex) from each poplar plant with liquid nitrogen at the following experimental phases: (1) before the experiments, (2) immediately after the experiment, i.e., after 24 hours of ISOPOOH fumigation (12 hours illuminated and 12 hours in the dark), and (3) 24 hours after the end of the enclosure experiment. The apparent *in vitro* AOR (alkenal/one oxidoreductase) activity was assessed as described in Yamauchi et al. (*45*). Frozen leaf material

was ground in liquid nitrogen using a dismembrator ball mill (B. Braun Biotech International, Melsungen, Germany). 200 mg of leaf powder were extracted in 4 ml of plant extraction buffer (100 mM Tris/HCl, pH 8.0, 20 mM $MgCl_2$, 100 mM $CaCl_2$, 1.5% PEG1500 (w/v), 5% (v/v) glycerol, 0.1% (v/v) Tween-20 and 20 mM DTT) with 200 mg polyvinylpolypyrrolidone (PVPP), stirred for 15 min on ice (4°C) and centrifuged for 15 min. at 20,000 *g*. The supernatant was purified on Sephadex G-25 PD-10 columns (GE Healthcare, Solingen, Germany) equilibrated with enzyme buffer (50 mM Tris/HCl, 20 mM $MgCl_2$, 5% (v/v) glycerol, 2 mM DTT) (*46*). Protein concentrations were determined by the Bradford assay using a Roti-Quant Kit (Carl Roth, Karlsruhe, Germany). Kinetics of AOR activity were measured in crude protein extracts in the presence of 0.15 mM NADPH, monitoring changes at A340 nm with a substrate concentration of 30 mM methyl vinyl ketone (MVK) (dissolved in enzyme buffer) against a control without MVK according to (*45*) in a final assay volume of 1 mL. From extracts of 7 (1,2-ISOPOOH fumigation) and 5 (MVK fumigation) biological replicates three technical replicates were measured. A description of the construction of the AOR phylogenetic tree and AOR gene expression analysis can be found in the SI Appendix.

The first *EC flux measurement* site is situated at the SMEAR II station in Hyytiälä, Finland. Vegetation around the site is dominated by Scots pine (*Pinus sylvestris*) with a canopy height of approximately 15 m. The ground level vegetation consists of lingonberry (*Vaccinium vitis-idaea*), blueberry (*V. myrtillus*) and mosses (*Pleurozium scheberi, Dicramum polysetum*) (*47*). Flux data for isoprene and MEK were obtained with the PTR3 using the eddy covariance (EC) method during spring 2016. The PTR3 sampled air through a specially designed 5 m long tube with a high flow rate on top of a 35 m tower. Wind speed measurements were taken 0.5 m above

353 the inlet opening by a METEK USA-1 sonic anemometer at 20 Hz. Wind direction and speed
354 were cross checked against the SMEAR II station instrumentation.
355
356 The second EC flux measurement site is situated at the University of Michigan Biological
357 Station (UMBS). Isoprene, MEK and other VOCs were measured by PTR-QiTOF as part of the
358 PROPHET-AMOS field study in July 2016 (*48*, *49*). The 34 m PROPHET tower (45.559 °N,
359 84.715°W, 232 m elevation) is located in a mixed deciduous/coniferous forest (canopy height
360 ~23 m) with an upper canopy dominated by aspen, birch and red oak and a lower canopy
361 consisting mainly of white pine, red maple, beech, and red oak (*50*, *51*). Net above-canopy VOC
362 fluxes were measured each hour by eddy covariance throughout the campaign. Sampling,
363 instrument operation, calibration procedures, data processing, and QA/QC are described in detail
364 elsewhere (*48*).
365
366 *GEOS-Chem* (v12.1.1, doi:10.5281/zenodo.2249246; www.geos-chem.org) is a global 3D CTM
367 driven by assimilated meteorological fields (Goddard Earth Observation System Forward
368 Processing product; GEOS-FP) from the NASA Global Modeling and Assimilation Office
369 (GMAO). The GEOS-FP data have native horizontal resolution of 0.25° latitude x 0.3125°
370 longitude with 72 vertical layers. For the year 2017 global simulations presented here, we
371 degrade the horizontal resolution to 2° x 2.5° and use a 15-min transport time step. We use the
372 TPCORE advection algorithm (*52*), convective mass fluxes from the GEOS-FP archive (*53*), and
373 the non-local boundary layer mixing scheme described by Lin and McElroy (*54*). Wet deposition
374 proceeds as described by Amos et al. (*55*). The default dry deposition in GEOS-Chem employs
375 the modified Wesely (1989) scheme (*9*) implemented by Wang et al. (*56*) with updated treatment

for OVOCs based on recent field constraints (*8*, *28*, *57*, *58*). Relevant parameters include H^* values of $1.7x10^6$ M/atm for 1,2-ISOPOOH and 44 M/atm for MVK. Reactivity (f_0) values for both species are set to 1.0.

The model includes comprehensive HO_x-NO_x-VOC-ozone-halogen chemistry coupled to aerosols and incorporates current JPL/IUPAC recommendations with recent updates for isoprene chemistry (*57*, *59*), peroxyacetyl nitrate (*60*) and Criegee chemistry (*61*). Photolysis frequencies are calculated using the Fast-JX algorithms developed by Bian and Prather (*62*, *63*). Biogenic VOC emissions are computed online based on the Model of Emissions of Gases and Aerosols from Nature (MEGANv2.1; (*2*)) as described by Hu et al. (*64*). Global anthropogenic emissions of VOCs, CO, NH_3, NO_x, SO_2 and aerosols are from the Community Emissions Data System (CEDS) inventory (*65*) overwritten by regionally specific inventories for North America (*66*), Asia (*67*) and Africa (*68*). Biogenic soil NO_x emissions are from Hudman et al. (*69*).

Data availability. The data that support the findings of this study are available from the corresponding author upon reasonable request.

References

1. A. H. Goldstein, I. E. Galbally, Known and unexplored organic constituents in the Earth's atmosphere. *Environ. Sci. Technol.* **41**, 1514–1521 (2007).

2. A. B. Guenther *et al.*, The model of emissions of gases and aerosols from nature version 2.1 (MEGAN2.1): An extended and updated framework for modeling biogenic emissions. *Geosci. Model Dev.* **5**, 1471–1492 (2012).

3. T. D. Sharkey, A. E. Wiberley, A. R. Donohue, Isoprene emission from plants: Why and how. *Ann. Bot.* **101**, 5–18 (2008).

4. A. T. Lantz, J. Allman, S. M. Weraduwage, T. D. Sharkey, Isoprene: New insights into the control of emission and mediation of stress tolerance by gene expression. *Plant. Cell Environ.* **42**, 2808–2826 (2019).

5. P. O. Wennberg *et al.*, Gas-phase reactions of isoprene and its major oxidation products. *Chem. Rev.* **118**, 3337–3390 (2018).

6. R. Atkinson, J. Arey, Gas-phase tropospheric chemistry of biogenic volatile organic compounds: a review. *Atmos. Environ.* **37**, 197–219 (2003).

7. A. P. Teng, J. D. Crounse, P. O. Wennberg, Isoprene peroxy radical dynamics. *J. Am. Chem. Soc.* **139**, 5367–5377 (2017).

8. T. B. Nguyen *et al.*, Rapid deposition of oxidized biogenic compounds to a temperate forest. *Proc. Natl. Acad. Sci.* **112**, E392–E401 (2015).

9. M. L. Wesely, Parameterization of surface resistances to gaseous dry deposition in regional-scale numerical models. *Atmos. Environ.* **23**, 1293–1304 (1989).

10. M. Wesely, A review of the current status of knowledge on dry deposition. *Atmos. Environ.* **34**, 2261–2282 (2000).

11. F. Paulot *et al.*, Unexpected epoxide formation in the gas-phase photooxidation of isoprene. *Science (80-.).* **325**, 730–733 (2009).

12. T. Berndt, N. Hyttinen, H. Herrmann, A. Hansel, First oxidation products from the reaction of hydroxyl radicals with isoprene for pristine environmental conditions. *Commun. Chem.* **2**, 21 (2019).

13. J. H. Seinfeld, S. N. Pandis, *Atmospheric chemistry and physics : from air pollution to climate change* (John Wiley & Sons, 2012).

14. H. J. H. Fenton, LXXIII.—Oxidation of tartaric acid in presence of iron. *J. Chem. Soc., Trans.* **65**, 899–910 (1894).

15. J. C. Rivera-Rios *et al.*, Conversion of hydroperoxides to carbonyls in field and laboratory instrumentation: Observational bias in diagnosing pristine versus anthropogenically controlled atmospheric chemistry. *Geophys. Res. Lett.* **41**, 8645–8651 (2014).

16. A. K. Bernhammer, M. Breitenlechner, F. N. Keutsch, A. Hansel, Technical note: Conversion of isoprene hydroxy hydroperoxides (ISOPOOHs) on metal environmental simulation chamber walls. *Atmos. Chem. Phys.* **17**, 4053–4062 (2017).

17. E. Chevallier, R. D. Jolibois, N. Meunier, P. Carlier, A. Monod, "Fenton-like" reactions of methylhydroperoxide and ethylhydroperoxide with Fe2+ in liquid aerosols under tropospheric conditions. *Atmos. Environ.* **38**, 921–933 (2004).

18. B. Sattelmacher, The apoplast and its significance for plant mineral nutrition. *New Phytol.* **149**, 167–192 (2001).

19. R. Mittler, Oxidative stress, antioxidants and stress tolerance. *Trends Plant Sci.* **7**, 405–410 (2002).

20. A. Polle, W. Junkermann, Inhibition of apoplastic and symplastic peroxidase activity from Norway Spruce by the photooxidant hydroxymethyl hydroperoxide. *Plant Physiol.* **104**, 617–621 (1994).

21. V. Shulaev, P. Silverman, I. Raskin, Airborne signalling by methyl salicylate in plant pathogen resistance. *Nature*. **385** (1997), pp. 718–721.

22. E. Rowen, M. Gutensohn, N. Dudareva, I. Kaplan, Carnivore attractant or plant elicitor? Multifunctional roles of methyl salicylate lures in tomato defense. *J. Chem. Ecol.* **43**, 573–585 (2017).

23. J. Kesselmeier, M. Staudt, Biogenic volatile organic compounds (VOC): An overview on emission , physiology and ecology. *J. Atmos. Chem.* **33**, 23–88 (1999).

24. J.-P. Schnitzler, S. Louis, K. Behnke, M. Loivamäki, Poplar volatiles - biosynthesis, regulation and (eco)physiology of isoprene and stress-induced isoprenoids. *Plant Biol.* **12**, 302–316 (2010).

25. A. Ghirardo *et al.*, Urban stress-induced biogenic VOC emissions and SOA-forming potentials in Beijing. *Atmos. Chem. Phys.* **16**, 2901–2920 (2016).

26. E. Alméras *et al.*, Reactive electrophile species activate defense gene expression in Arabidopsis. *Plant J.* **34**, 205–216 (2003).

27. H. Esterbauer, R. J. Schaur, H. Zollner, Chemistry and biochemistry of 4-hydroxynonenal, malonaldehyde and related aldehydes. *Free Radic. Biol. Med.* **11**, 81–128 (1991).

28. T. Karl *et al.*, Efficient atmospheric cleansing of oxidized organic trace gases by vegetation. *Science (80-.).* **330**, 816–819 (2010).

29. S. Muramoto *et al.*, Glutathionylation and reduction of methacrolein in tomato plants account for its absorption from the vapor phase. *Plant Physiol.* **169**, 1744–1754 (2015).

30. L. Cappellin *et al.*, Field observations of volatile organic compound (VOC) exchange in red oaks. *Atmos. Chem. Phys.* **17**, 4189–4207 (2017).

31. L. Cappellin, F. Loreto, F. Biasioli, P. Pastore, K. McKinney, A mechanism for biogenic production and emission of MEK from MVK decoupled from isoprene biosynthesis.

Atmos. Chem. Phys. **19**, 3125–3135 (2019).

32. P. Wanner, R. Tressl, Purification and characterization of two enone reductases from Saccharomyces cerevisiae. *Eur. J. Biochem.* **255**, 271–278 (1998).

33. A. Kergomard, M. F. Renard, H. Veschambre, D. Courtois, V. Petiard, Reduction of α,β-unsaturated ketones by plant suspension cultures. *Phytochemistry*. **27**, 407–409 (1988).

34. Y. Yamauchi, A. Hasegawa, M. Mizutani, Y. Sugimoto, Chloroplastic NADPH-dependent alkenal/one oxidoreductase contributes to the detoxification of reactive carbonyls produced under oxidative stress. *FEBS Lett.* **586**, 1208–1213 (2012).

35. E. Georgii *et al.*, The systems architecture of molecular memory in poplar after abiotic stress. *Plant Cell*. **31**, 346–367 (2019).

36. H. B. Singh *et al.*, Analysis of the atmospheric distribution, sources, and sinks of oxygenated volatile organic chemicals based on measurements over the Pacific during TRACE-P. *J. Geophys. Res. D Atmos.* **109** (2004), doi:10.1029/2003JD003883.

37. M. Breitenlechner *et al.*, PTR3: An instrument for studying the lifecycle of reactive organic carbon in the atmosphere. *Anal. Chem.* **89**, 5824–5831 (2017).

38. H. B. Singh, M. Kanakidou, P. J. Crutzen, D. J. Jacob, High concentrations and photochemical fate of oxygenated hydrocarbons in the global troposphere. *Nature*. **378**, 50–54 (1995).

39. J. F. Brewer *et al.*, Atmospheric Photolysis of Methyl Ethyl, Diethyl, and Propyl Ethyl Ketones: Temperature- Dependent UV Absorption Cross Sections. *J. Geophys. Res. Atmos.* **124**, 2019JD030391 (2019).

40. M. E. Jenkin, S. M. Saunders, M. J. Pilling, The tropospheric degradation of volatile

organic compounds: a protocol for mechanism development. *Atmos. Environ.* **31**, 81–104 (1997).

41. J. F. Brewer *et al.*, Evidence for an Oceanic Source of Methyl Ethyl Ketone to the Atmosphere. *Geophys. Res. Lett.* **591**, 5022–5024 (2020).

42. M. Graus, M. Müller, A. Hansel, High resolution PTR-TOF: quantification and formula confirmation of VOC in real time. *J. Am. Soc. Mass Spectrom.* **21**, 1037–44 (2010).

43. M. Müller, T. Mikoviny, W. Jud, B. D'Anna, A. Wisthaler, A new software tool for the analysis of high resolution PTR-TOF mass spectra. *Chemom. Intell. Lab. Syst.* **127**, 158–165 (2013).

44. E. Vanzo *et al.*, Modulation of protein S -nitrosylation by isoprene emission in poplar. *Plant Physiol.* **170**, 1945–1961 (2016).

45. Y. Yamauchi, A. Hasegawa, A. Taninaka, M. Mizutani, Y. Sugimoto, NADPH-dependent reductases involved in the detoxification of reactive carbonyls in plants. *J. Biol. Chem.* **286**, 6999–7009 (2011).

46. J. P. Schnitzler *et al.*, Biochemical properties of isoprene synthase in poplar (*Populus x canescens*). *Planta*. **222**, 777–786 (2005).

47. H. Ilvesniemi, R. Giesler, P. Van Hees, T. Magnussson, P. A. Melkerud, General description of the sampling techniques and the sites investigated in the Fennoscandinavian podzolization project. *Geoderma*. **94**, 109–123 (2000).

48. D. B. Millet *et al.*, Bidirectional ecosystem-atmosphere fluxes of volatile organic compounds across the mass spectrum: How many matter? *ACS Earth Sp. Chem.* **2**, 764–777 (2018).

49. H. D. Alwe *et al.*, Oxidation of volatile organic compounds as the major source of formic acid in a mixed forest canopy. *Geophys. Res. Lett.* **46**, 2940–2948 (2019).

50. A. M. Bryan *et al.*, Forest-atmosphere BVOC exchange in diverse and structurally complex canopies: 1-D modeling of a mid-successional forest in northern Michigan. *Atmos. Environ.* **120**, 217–226 (2015).

51. B. J. Palik, K. S. Pregitzer, A comparison of presettlement and present-day forests on two bigtooth aspen-dominated landscapes in Northern Lower Michigan. *Am. Midl. Nat.* **127**, 327 (1992).

52. S.-J. Lin, R. B. Rood, Multidimensional flux-form semi-Lagrangian transport schemes. *Mon. Weather Rev.* **124**, 2046–2070 (2002).

53. X. Wu, L. Deng, X. Song, G. J. Zhang, Coupling of convective momentum transport with convective heating in global climate simulations. *J. Atmos. Sci.* **64**, 1334–1349 (2007).

54. J.-T. Lin, M. B. McElroy, Impacts of boundary layer mixing on pollutant vertical profiles in the lower troposphere: Implications to satellite remote sensing. *Atmos. Environ.* **44**, 1726–1739 (2010).

55. H. M. Amos *et al.*, Gas-particle partitioning of atmospheric Hg(II) and its effect on global mercury deposition. *Atmos. Chem. Phys.* **12**, 591–603 (2012).

56. Y. Wang, J. A. Logan, D. J. Jacob, Global simulation of tropospheric O_3 -NO_x-hydrocarbon chemistry: 2. Model evaluation and global ozone budget. *J. Geophys. Res. Atmos.* **103**, 10727–10755 (1998).

57. K. R. Travis *et al.*, Why do models overestimate surface ozone in the Southeast United States? *Atmos. Chem. Phys.* **16**, 13561–13577 (2016).

58. E. A. Marais *et al.*, Aqueous-phase mechanism for secondary organic aerosol formation from isoprene: application to the southeast United States and co-benefit of SO_2 emission controls. *Atmos. Chem. Phys.* **16**, 1603–1618 (2016).

59. J. A. Fisher *et al.*, Organic nitrate chemistry and its implications for nitrogen budgets in an isoprene- and monoterpene-rich atmosphere: Constraints from aircraft (SEAC 4 RS) and ground-based (SOAS) observations in the Southeast US. *Atmos. Chem. Phys.* **16**, 5969–5991 (2016).

60. E. V. Fischer *et al.*, Atmospheric peroxyacetyl nitrate (PAN): a global budget and source attribution. *Atmos. Chem. Phys.* **14**, 2679–2698 (2014).

61. D. B. Millet *et al.*, A large and ubiquitous source of atmospheric formic acid. *Atmos. Chem. Phys.* **15**, 6283–6304 (2015).

62. H. Bian, M. J. Prather, Fast-J2: Accurate simulation of stratospheric photolysis in global chemical models. *J. Atmos. Chem.* **41**, 281–296 (2002).

63. S. D. Eastham, D. K. Weisenstein, S. R. H. Barrett, Development and evaluation of the unified tropospheric-stratospheric chemistry extension (UCX) for the global chemistry-transport model GEOS-Chem. *Atmos. Environ.* **89**, 52–63 (2014).

64. L. Hu *et al.*, Isoprene emissions and impacts over an ecological transition region in the U.S. Upper Midwest inferred from tall tower measurements. *J. Geophys. Res.* **120**, 3553–3571 (2015).

65. R. M. Hoesly *et al.*, Historical (1750–2014) anthropogenic emissions of reactive gases and aerosols from the Community Emissions Data System (CEDS). *Geosci. Model Dev.* **11**, 369–408 (2018).

66. EPA, 2011 National Emissions Inventory Data & Documentation (2015), (available at https://www.epa.gov/air-emissions-inventories/2011-national-emission-inventory-nei-report).

67. M. Li *et al.*, MIX: A mosaic Asian anthropogenic emission inventory under the international collaboration framework of the MICS-Asia and HTAP. *Atmos. Chem. Phys.* **17**, 935–963 (2017).

68. E. A. Marais, C. Wiedinmyer, Air quality impact of Diffuse and Inefficient Combustion Emissions in Africa (DICE-Africa). *Environ. Sci. Technol.* **50**, 10739–10745 (2016).

69. R. C. Hudman *et al.*, Steps towards a mechanistic model of global soil nitric oxide emissions: Implementation and space based-constraints. *Atmos. Chem. Phys.* **12**, 7779–7795 (2012).

Acknowledgement

The authors would like to thank Bernhard Mentler (UIBK) for developing the ISOPOOH and IEPOX measurement protocol using different reagent ions, Ulrich Junghans (Helmholtz) for growing the sample plants, Frank Keutsch & Jean Rivera-Rios (Harvard University) for providing the 1,2-ISOPOOH standard and Holger Kopacka (UIBK) for the NMR analysis of the samples. We thank Xin Chen (UMN) for assistance with the model simulations, along with Steven Bertman (WMU) and the entire PROPHET-AMOS team for their support and contributions to the field campaign. We thank Martin Breitenlechner (UIBK) for contributions to the Hyytiälä field campaign. We thank the Institute of Microbiology from the University of Innsbruck for sharing the greenhouse facility.

Funding

This study was supported by the Austrian Federal Ministry of Education, Science and Research within Sparkling Science (grant SPA 05/080 - AiR and grant SPA 06/222 - CHAMPIONS). VOC flux measurements at Hyytiälä were supported by the European Commission under Horizon 2020, (H2020-INFRAIA-2014-2015, grant 654109, ACTRIS). VOC measurements during PROPHET were supported by the US National Science Foundation (NSF grants AGS-1428257 and AGS- 1148951). GEOS- Chem model development and simulations were supported by the US National Aeronautics and Space Administration (NASA grant NNX14AP89G). Computing resources at UMN were provided by MSI (www.msi.umn.edu).

Author contributions

AH, EC and JPS designed the experiment. EC, EP performed the laboratory measurements and data analysis, LF assisted with data analysis. IZ and JPS measured AOR activities. TN, EG and JPS generated the AOR phylogenesis. DBM, HDA, and LF contributed with eddy flux data. DBM ran the GEOS-Chem model and analyzed the results. WJ and TK took part in data discussion and manuscript improvement. The manuscript was written through contributions of all authors. All authors have given approval to the final version of the manuscript.

Additional information

Supplementary information is available in the online version of the paper.

Competing interests

Authors declare no competing interests.

Point-by-point response to the reviewer comments:

First of all, we would like to thank both reviewers for thoroughly reviewing our manuscript and for their comments that helped to improve the manuscript. Our responses to the reviewer comments are below.

Reviewer #1 (Remarks to the Author):

This is a very nice study were 1,2-ISOPOOH reaction with poplar plants were shown to produce MEK and MVK in equal quantities.
the work if of great interest for the community as it proposes a process of MEK biogenic "catalysis" from 1,2-ISOPOOH. The authors propose a mechanism in which alkenal/one oxidoreductase (AOR) is responsible for that process. They then evaluate globally the amount of MEK may be formed by this process

The science is excellent and the experiments use state of the art instruments.

However some conclusions may be raised without being very solid to my point and some causality link may be missing:

1. The role of AOR in forming MEK from MVK is likely but not demonstrated per se in this study. The activity of this enzyme does not change with the dose of 1,2-ISOPOOH.

   Response: We measured the enzyme activity of AOR in protein extracts of poplar leaves, which were used for the deposition studies. This was preceded by a characterization of the in vitro enzyme activity to determine the biochemical properties. The in vitro activity of the AOR was then measured (under optimal substrate conditions) at the same temperature as in the deposition studies. The measurements show that poplar leaves are able to reduce MVK to MEK with a dependence on NADPH as an electron donor. During the short time after application of ISOPOOH and MVK no increase in enzyme activity was observed. This may be due to the fact that the observation time period was too short to capture the ensuing activation of the enzyme activity. However, it is also possible that the constitutively present amount of enzyme is sufficient to catalyze the observed conversion from MVK to MEK.
   Furthermore, the AOR belongs to a group of enzymes that are post-translationally modified (PTM) by S-nitrosylation on cysteines (see (Vanzo et al., 2015)). This modification can lead to a short-term change in “in-vivo” enzyme activity without a change in protein amount via transcription/translation.
   For information on this we have included a new Supplementary Figure 12.
   We agree with the reviewer that on the basis of the available measurements no absolute causal but only a correlative relationship can be established. A conclusive relationship can only be tested in transgenic plants in which the transcription of the gene encoding for this enzyme is either completely blocked or overexpressed. However, experiments with such plants are only feasible in the long term, since the production of such lines requires about 1-2 years.

2. The location of the conversion is assumed to be the apoplasm, but this is also not stricktly demonstrated: indeed ISOPOOH is water soluble but cuticles show a microscopic layer which is wet when stomata open: it may well be that the reaction takes place on the leaves surfaces but not in the apoplasm.

   Response: Our measurement protocol aimed answering the important question of what happens to highly water soluble 1,2-ISOPOOH at the leaf surface. We observed strongly increased 1,2-ISOPOOH uptake when switching on the light (shown in the manuscript).

Under daylight conditions stomata are open as confirmed by the change in CO_2. We thus inferred that the increased 1,2-ISOPOOH uptake occurred via stomatal uptake. Strictly speaking, a light-induced loss of 1,2-ISOPOOH at the leaf surface could also explain such findings. In early experiments, we used unrealistically high 1,2-ISOPOOH concentrations (these were not used subsequently for results shown in the paper as submitted). Interestingly, this high-level 1,2-ISOPOOH fumigation over several hours stressed one plant so much that stomata closed under lit conditions. The stomatal closing was accompanied by an increase of 1,2-ISOPOOH, while MVK levels remained nearly unchanged and MEK levels decreased. This indicates that the 1,2-ISOPOOH conversion proceeds strongly when stomata are open and 1,2-ISOPOOH enters the plant.

To address this point we have included a new Supplementary Figure 6.

We have also included the following text in the manuscript:

Supplementary Figure 6 shows an experiment with a poplar plant exposed to elevated 1,2-ISOPOOH in the presence of light. Stomatal closure is observed, likely due to stress. Upon stomatal closure, 1,2-ISOPOOH levels in the enclosure increase, indicating that stomatal uptake is the dominant loss process and not light-induced plant surface uptake.

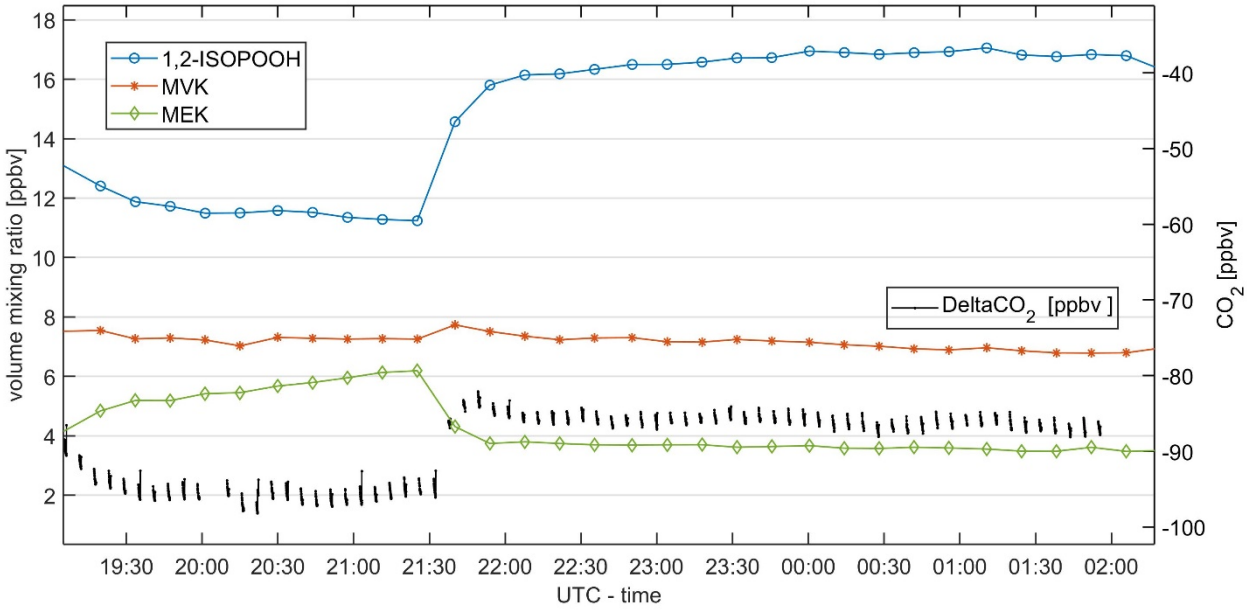

3. The worldwide evaluation should be more justified and explained: the use of the laboratory deposition velocity should be more explicited, and the fact that experiments with poplars are used to generate worldwide estimates also justified. Although the enzyme AOR is ubiquitous, its content will change with plants and its activity probably with temperature. This should be discussed.

Response: The worldwide evaluation should be more justified and explained:

For many years scientists have used plant enclosure experiments in combination with field-based flux measurements to better asses global BVOC emissions. For example, (Guenther et al. (1996) compared BVOC flux estimates from enclosure and ambient measurements and found agreement to within a factor of two. In recent years CIMS instruments have became increasingly sensitive, and now permit direct eddy covariant (emission and deposition) flux measurements above different ecosystems.

We know that eddy covariant deposition fluxes of ISOPOOH and MVK are difficult to measure even with the most sophisticated CIMS instruments. 1,2-ISOPOOH has an interference with its isomer IEPOX and also decomposes on metal surfaces to MVK. As a solution to this analytical challenge we performed well-characterized plant enclosure measurements to obtain deposition velocities of these challenging species in the laboratory. These deposition velocities were then implemented in an updated version of the GEOS-Chem chemical transport model. Our approach also included direct eddy covariant flux measurements utilizing state of the art instrumentation above two different ecosystems. We used field-calibrated emission fluxes of isoprene and MEK (which can be reliably obtained) and found good agreement with the MEK : isoprene flux ratio predicted by the modified GEOS-Chem model.

We have now clarified the description of how laboratory deposition velocities were used in the GEOS-Chem simulations by including the following text in the manuscript:
Instead, we prescribe the modeled 1,2-ISOPOOH and MVK deposition velocities over land based on the results from our laboratory measurements employing constant daytime (nighttime) deposition velocities of 0.22 (0.014) cm s^{-1} for MVK and 0.79 (0.1) cm s^{-1} for 1,2-ISOPOOH. Over oceans the default model scheme is used.

In addition, the GEOS-Chem model description has been improved as suggested.
The updated text is highlighted in the manuscript.

The reviewer asked us to justify the use of poplar plants to generate worldwide estimates.

***Response**: We have now inserted the following text in the manuscript.*
"Poplars occur worldwide, both in natural forests and plantations, and are among the most globally important boreal deciduous tree species. In plant science, poplars represent the most important model system for tree research and were the first tree species for which the genome was described. Many studies, in particular for VOCs, show that the biological and physiological processes studied in poplars can be transferred to other tree species (e.g. (Baldwin and Schultz, 1983; Sharkey et al., 2008). Poplar plants several months in age were selected for the present work because they allow gas exchange analyses and deposition experiments to be carried out in a very well controlled and reproducible manner. Many VOC emission studies have shown that such results can be transferred to older trees and can hence be used for modelling studies on regional and global scales (e.g. (Guenther et al., 2012; Monson et al., 2020))."

Previous proteome and transcriptome analyses of poplars also provided basic knowledge about the AOR. In the course of establishing the AOR enzyme assay, the biochemical properties of the AOR were determined. In addition to the dependence on the substrates NADPH and MVK, the temperature dependence of the in vitro activity was tested. The AOR activity increases with temperature, reaching a maximum at 35°C and then decreasing. This is now summarized in the new Supplementary Figure 9 and described in the manuscript.

I think that this manuscript should be published but with more discussions on the points above.

Comments of Reviewer 1 regarding the main manuscript:

- Line 37: "… why plants emit isoprene …" There might be no "reason", but just a minor drawback of a useful process linked with diffusion?
    - We changed the sentence to "… the question of why plants emit isoprene is still not fully understood".
- Line 68: "… (see Methods for details)."
    - Please see our reply to the later related comment; additional details have been added to this section of Methods.
- Figure 1: Could these reactions also happen within the canopy?
    - Isoprene lifetime due to OH is 1.4 hours assuming an OH concentration of 2 x 10^6 radicals cm^{-3}. Due to rather short residence time of air parcels (minutes) and lower OH concentration within canopy isoprene is primarily oxidized in the atmosphere above the canopy.
- Line 96: Give untis.
    - We added units.
- Line 99: Actually in the SI it is rather ci,out,bgd that is used rather than ci,out. Please make it coherent.
    - We changed it to the nomenclature used in the SI.
- Strictly speaking you did not show that exactly, but it is a very likely possibility indeed. But could you argue on why it is not likely that a plant surface reaction takes place when light is turned on? Moreover it was well shown by early work on cuticles that these may be totally wet even in relatively dry conditions as soon as the stomata are open. This is a well-known feature for ammonia deposition. Please have a look at these studies:
  Burkhardt, J. and Eiden, R., 1994. Thin Water Films on Coniferous Needles. Atmos. Environ., 28(12): 2001-2011. Fuentes, J.D., Gillespie, T.J. and Bunce, N.J., 1994. Effects of foliage wetness on the dry deposition of ozone onto red maple and poplar leaves. Water, Air, and Soil Pollution, 74(1): 189-210. Burkhardt, J., 1995. Hygroscopic salts on the leaf surface as a possible cause of forest decline symptoms. Water Air and Soil Pollution, 85(3): 1245-1250. Flechard, C.R., Fowler, D., Sutton, M.A. and Cape, J.N., 1999. A dynamic chemical model of bi-directional ammonia exchange between semi-natural vegetation and the atmosphere. Q.J.R. Meteorol. Soc., 125(559): 2611-2641. Zhang, L., Brook, J.R. and Vet, R., 2002. On ozone dry deposition-with emphasis on non-stomatal uptake and wet canopies. Atmos. Environ., 36: 4787-4799.
    - Please see our earlier response to question 2.
- Line 130: Strictly speaking it was not demonstrated here that this is happening in the apoplasm. wet cuticle may be also the location.
    - We added Supplementary figure 6 to support our assumption. Figure S 6 shows an experiment with induced stomatal closure during light conditions. 1,2-ISOPOOH mixing ratios rapidly increased while MEK levels declined, supporting our contention that 1,2-ISOPOOH is mainly converted in the apoplast.
- Line 150: Would such transition metals be present on leaves surfaces?
    - To our knowledge no studies about this topic exist. Possibly metal containing nanoparticles could be deposited to leaf surfaces.
- Line 165: And did you see any MACR emissions then?
    - We used NO^+ reagent ions to separate MACR from MVK. We see small amounts of MACR, but MACR levels did not change while fumigating with 1,2-ISOPOOH under light and dark conditions.
- Line 172: Could you remind how this was clearly shown by your data?
    - We clarified the statement by adding the following sentence to the manuscript: "We characterized the in vitro kinetic properties of the poplar AOR (EC 1.3.1.74) enzyme to which we attribute the in planta conversion of MVK to MEK. We obtain Michaelis-Menten constants (substrate concentration at half-maximal enzyme velocity) of 0.049 mM and 14.15 mM for NADPH and MVK, respectively, and a temperature optimum at 35°C (Fig. S 9)."
- Line 184: So how do you make the link between its activity and MVK conversion?

- We added the following paragraph to the manuscript: “The fact that we do not see any change to the in situ AOR activity as a result of exposure to 1,2-ISOPOOH and MVK (Fig. S10) may be due to the fact that our observation period was too short and missed a stress-induced response. However, AOR also belongs to a group of proteins that are post-translationally modified (PTM) by S-nitrosylation at certain cysteine residues under stress (Figure S12, Vanzo et al. 2015), which may change in vitro enzyme activity. In planta, i.e. the intact leaves as we used for the gas exchange analyses, AOR activity is variable depending on actual leaf temperature, light energy providing electrons in the form of NADPH for the reduction of MVK to MEK, and the presence of MVK, which is provided by deposition or degradation of 1,2-ISOPOOH.”

- Line 211: But how exactly? Is that a daily variation? A light dependence?
  - We have clarified this point in the manuscript as requested: “Instead, we prescribe the modeled 1,2-ISOPOOH and MVK deposition velocities over land based on the results from our laboratory measurements employing constant daytime (nighttime) deposition velocities of 0.22 (0.014) cm s^{-1} for MVK and 0.79 (0.1) cm s^{-1} for 1,2-ISOPOOH. Over oceans the default model scheme is used.”

- Line 214: Well aerodynamic resistance plays anyway a role and adds up to the surface resistance. It should not be one or another.
  - Yes, we agree. The text reads now:
    “... uptake for these compounds is controlled by surface and molecular diffusion resistance, an assumption strongly supported by prior work (Nguyen et al., 2015).“
- Line 218: Since you talk about dry deposition it means you account for both cuticulat and stomatal now. Is that the case?
  - Yes, that is the case.
- Line 268: Well there are still points to demonstrate: - AOR implication in the process is not strictly demonstrated - localisation: apoplast versus cuticle+ light reaction still needs to be demonstrated.
  - As described above we have now strengthened this argument by adding figure S6 and additional descriptions of the AOR analysis in the main text.
- Line 319: Were they washed to get rid of particles likely deposited on their leaves especially in greenhouse with no rain. These particles may have reacted with ISOPOOH under light and hence wet conditions.
  - We did not wash the poplars prior to the experiments to avoid changes in the chemical composition of the surface. Therefore, we cannot exclude effects of possible aerosols on the leaf surfaces. But our experiments indicate that ISOPOOH conversion takes places mainly in the apoplast (see figure S6) and is strongly light-induced. Thus, we assume that effects on the surfaces play a minor role.

Comments of Reviewer 1 regarding the Supplementary Material

- Page 3: Please give a reference to justify using this equation for calculating the deposition rate.
  - We added the reference.
- Page 4: One important point is if the leaves were washed before the experiment to get rid of possible particles sitting on the cuticles that may have affect surface water content and the presence of metals there. See references proposed in comments.
  - Please see our response to the earlier comment.
- Page 5: I am not sure this is equivalent to the integration of the mass conservation equation in the volume accounting for kdep? Could you give a reference that shows it is equivalent or alternatively show the link in equations.
  - We added the reference in the text.
- Page 7: Could you precise what is the water sensitive tracer?

- We used N_2H^+ as a fast water-sensitive tracer.

- Page 13: How did you account for the non steady conditions in C after 60 minutes? How do you explain them?
  - Switching on the light leads to non-steady state conditions. The humidity increases strongly and the plant stomata open. ISOPOOH is taken up by the plant. MVK and MEK signals increase. We didn't use data during this time span for analysis.
- Page 14: It would be good to show significance on that graph with an appropriate statistical test. Tukey may be?
  - We performed a Tukey post hoc analysis test and added statistical analysis in the figure caption.
- Page 17: This is not strictly speaking an emission but a relative change in % of the PTR signal. Isn't?
  - Due to a lack of calibration gas standards we plotted the relative ion signals. We changed the figure title and the text in the caption.
- Page 19: I am not sure what this figure is intended for. To me it seems to show that there is no significant in AOR activity between exposure durations. Is it really necessary? If so should you may be show significance between periods?
  - We agree with the reviewer. But in the text we refer to the data presented. Therefore we keep the figure at this point.
- Page 20: Why is the stomatal fraction of ISOPOOH deposition so high in northern Asia and Canada?
  - We believe the reviewer is referring here to Figure S14, which shows the MEK production divided by isoprene emissions (the stomatal fraction of 1,2-ISOPOOH deposition in Figure S13 does not show particularly elevated values in north Asia or north Canada). The high MEK yields in Figure S14 in those locations reflect the low OH levels, which lead to a larger fraction of MVK and 1,2-ISOPOOH undergoing dry deposition rather than being photo chemically oxidized. In turn this leads to a higher MEK yield per unit isoprene emission. However, the isoprene emissions and absolute MEK production rates are quite low in those areas, as shown in Figure 4. We have added text to the Figure S14 caption to clarify this point: "Elevated values are seen where OH is low and isoprene oxidation products undergo proportionately more deposition (e.g., high latitudes), and in low-emission locations subject to deposition from nearby high-emission areas (e.g., western South America)."
- Page 20: Could you explain how it is calculated or make reference to a manuscript?
  - We have added more information to the Figure S13 caption as requested: "Values plotted reflect the stomatal fraction of deposition (i.e., stomatal conductance divided by total surface conductance) as a conductance-weighted mean across all land cover types within each model grid cell."
- Page 21: Enzymes activity are temperature dependent. Was that taken into account for instance in northern latitudes? Why is that so high in cold environment?
  - It is rather a question of atmospheric chemistry than enzymatic activity. Please see our reply to an earlier comment on page 20.

Reviewer #2 (Remarks to the Author):

The paper describes a new finding that ISOPOOH is quickly converted to MVK and MEK by plants and shows global emission estimate of MEK, using data including laboratory fumigation measurement, field flux measurement and global estimate model. It is worth being published by the journal after revisions described below are carefully conducted by the authors.

Fig. 2 title
Which concentration are they? inlet or outlet? except “inlet”, the other three seem to be outlet. If so, mention this.

> ***Response:*** Only “inlet” was measured in the inlet. We now indicate in Fig. 2 that the other three (BG, dark, and light) were measured at the “outlet”

Line 154 S. Muramoto et al. (29) did not show the relationship between stomatal opening and uptake of MVK. More accurate measurement was done by Tani et al (Environmental Science & Technology 44, 7096-7101. 2010) at low concentration of MVK and MAC. They showed a clear relationship between stomatal conductance and MVK uptake rate. They show MEK source is also plants. Please check it and consider to cite it.

> ***Response:*** We thank the reviewer for pointing out the importance of Tani et al. (2010), we were not aware. They used atmospherically relevant mixing ratios of MVK and MACR and their uptake rates are similar to our values. We added this reference in line 157.

It is better to globally estimate plant uptake of MEK in addition to MEK emission, as MEK is the second abundant ketone beside acetone. MEK is absorbed by all plants including non-isoprene emitters in the world. In Fig 4, you need to add the estimate of MEK deposition onto forests. This process is also governed by stomata. If it is difficult to do this, at least mention the importance of MEK deposition onto terrestrial ecosystem by citing the papers below. These papers indicate that MEK source is also plants. (Tani et al., 2010, Environmental Science & Technology 44, 7096-7101.; Tani et al., 2013, Atmospheric Environment 70, 300-306.; Cappellin et al., Atmospheric Chemistry and Physics 2019, 19, 3125-3135).

> ***Response:*** Modifying Figure 4 in this way is indeed not simple as it requires additional model development to incorporate the additional MEK source from MVK+ISOPOOH in order to then estimate the resulting total MEK deposition. We have therefore taken the reviewer’s alternate suggestion to mention the importance of MEK deposition with appropriate citations: “… making this mechanism the largest known MEK source to the atmosphere (36). In turn, a fraction of that MEK will return to the ecosystem via further dry deposition (e.g., Tani et al., 2010; Tani et al., 2013; Cappellin et al., 2019).”

Line 245 How did you distinguish MEK from isomers including butanal and 2-methy propanal. They are also ubiquitous. Here you used proton-transfer reaction using H3O+? Explain it in more detail in the MS.

> ***Response:*** We added a more detailed description of the SRI-TOF-MS instrument in the Supplementary Information: To distinguish MEK from isomers such as butanal and 2-methyl propanal, we used the reagent ion NO^+. Our instrument allows fast switching between different reagent ions. According to (Španěl et al., 2002) the two isomers butanal and 2-methyl propanal undergo hydride abstraction forming the product ion $C_4H_7O^+$. In contrast, MEK reacts with NO^+ via an association reaction forming $C_4H_8O\text{-}NO^+$.

Line 317 Show plant detail in material section, at least shoot dry weight and leaf area.

> ***Response:*** We added a table (Supplementary Table 5) with plant details in the supplementary material. Shoot dry weight is not available.

Line 319 You cannot extrapolate the uptake rate obtained using such infant trees to ecosystem scale. How do you link such infant tree results to adult tree one?

Response: We have inserted the following text in the manuscript.
"Poplars occur worldwide, both in natural forests and plantations, and are among the most important boreal deciduous tree species. In plant science, poplars represent the most important model system for tree research in plant sciences and were the first tree species for which the genome was described. Many studies, in particular for VOCs, show that the biological and physiological processes studied in poplars can be transferred to other tree species (e.g. (Baldwin and Schultz, 1983; Sharkey et al., 2008). Poplar plants several months in age were selected for the present work because they allow gas exchange analyses and deposition experiments to be carried out in a well-controlled and reproducible manner. Many VOC emission studies have shown that such results can be transferred to older trees and can hence be used for modelling studies on regional and global scales (e.g. (Guenther et al., 2012; Monson et al., 2020))."

Line 372-389 As the description here is mostly dependent on citation, readers cannot understand the method. No supporting information is given for this part. More detailed explanation should be given in MS or SI. Especially explant how to estimate MEK emission and what deposition data of MEK including deposition velocity is basically used.

Response: We aim to keep the Methods concise to avoid simply repeating information that is already published elsewhere. However, to address the reviewer's general comment we have now added some additional details to this part of the Methods section. Please note that we do not compute or show in the paper MEK deposition fluxes so we have not added information on this specific topic to the Methods.

In supporting information 6
Line 2 In Representative poplar fumigation experiment
"In step A, we enriched the air with 7.8±1.0 ppbv of 1,2-ISOPOOH across all replicates."
The mixing ratio seems to be high if we see natural environment. It may be difficult to set it below ppbv, but authors need to explain how to extrapolate this uptake and emission results to terrestrial ecosystem.

Response: In the low-NO atmosphere ISOPOOH reaches values of up to 2 ppbv during daylight hours. (Worton et al., 2013) measured up to 2 ppbv ISOPOOH during the BEARPEX experiments in the Sierra Nevada Mountains (US). We enriched the enclosure inlet air with 7-8 ppbv of 1,2-ISOPOOH resulting in ~6 ppbv under dark and ~ 3 ppbv under light conditions in the enclosure outlet air (Supplementary Figure 3), which is very close to the 2 ppbv measured during BEARPEX. We used the slightly higher values as a compromise of being close to natural values and reducing measurement errors. As described in Methods our glass enclosure surfaces were specially treated with Teflon to be as inert as possible, and for every experiment wall losses were characterized. ISOPOOH needs some time to establish a new equilibrium when concentrations are changed.

In Experimental design

"The plants were fumigated with synthetic air (5.0 grade, Messer Austria GmbH, Gumpoldskirchen, Austria) that was mixed with CO2 (4.8 grade, Messer Austria GmbH, Gumpoldskirchen, Austria)" The air and pure CO2 are not perfectly pure, possibly including other compounds that may interfere the measurement. Authors need to check the contamination level of the air before doing experiment using GCMS.

Response: Thank you for raising this important question. We have now added a new paragraph in the Supplementary Information entitled "Impurity determination for fumigation experiments":
For all fumigation experiments we used a 12-bottle bundle of synthetic air (5.0 grade). This synthetic air contains < 0.1 ppmv hydrocarbons (as CH_4) and the largest contamination is water

vapor (< 5 ppmv). For each plant experiment we conducted a "blank" measurement of the empty enclosure. The SRI-TOF-MS limit of detection (LOD) for MVK and MEK was 0.03 ppbv, while the LOD for 1,2-ISOPOOH was 0.21 ppbv. Blank measurements of the empty enclosure with humidified synthetic air containing 480 ppm CO_2 revealed contaminants at m/z 88.07 (C_4H_6O-NH_4^+, MVK) and m/z 90.09 (C_4H_8O-NH_4^+, MEK) of 0.09 ppbv and 0.07 ppbv, respectively. Contaminants at m/z 136.09 ($C_5H_{10}O_3$-NH_4^+, 1,2-ISOPOOH) were below the detection limit. During plant enclosure experiments observed ion signals are substantially higher than these background signals.

In "Representative poplar fumigation experiment"
How did you avoid water vapor condensation onto inner surface of the enclosure bag?

Response: To avoid water vapor condensation on the inner surface of the enclosure we used a temperature controlled water bath located between the daylight lamp and the glass enclosure to filter infrared radiation. Additionally we adapted the inlet flow to the leaf area of the fumigated plant. The air in the enclosure was constantly mixed turbulently by a fan.

In "Infrared gas analyzer (IRGA)"
What is the flow rate to IRGA? Especially water vapor is also sticky and needs to relatively high flow rate.

Response: The infrared gas analyzer LI-840A must be continually flushed with 0.25 to 1 liters per minute. During all experiments we flushed the IRGA with 0.5 to 1 liters per minute.

Equation (4) and (5) The equations are not correct in this case. The outlet air is more humidified by plant transpiration and the flow rate F is not same between the inlet and outlet, usually 1-2% higher in the outlet. You need to add humidity-correction term in the equation. The paper shown below is source of the equation and refer it please.
von Caemmerer, S.; Farquhar, G. D. Some relationships between the biochemistry of photosynthesis and the gas exchange o leaves. Planta 1981, 153 (4), 376–387.

Response: The flow rate at the enclosure outlet was lower than the inlet flow rate leading to an enclosure pressure slightly higher than ambient. With this approach we can exclude any possibility of room air leaking into the enclosure. As recommended by the reviewer we have applied the humidity correction term to our data and derive slightly changed 1,2-ISOPOOH deposition velocities of 0.12 ± 0.04 cm s^{-1} (dark conditions) and 0.79 ± 0.25 cm s^{-1} (light conditions). The humidity corrected day time deposition value is increased by 1.3%.
For MVK we also applied the humidity correction and derived slightly changed deposition velocities of $v_d = 0.044 \pm 0.045$ cm s^{-1} (dark conditions) and 0.22 ± 0.17 cm s^{-1} (light conditions).

References

Baldwin, I. T., and Schultz, J. C. (1983). Rapid Changes in Tree Leaf Chemistry Induced by Damage: Evidence for Communication Between Plants. *Science (80-.).* 221, 277–279. doi:10.1126/science.221.4607.277.

Guenther, A. B., Jiang, X., Heald, C. L., Sakulyanontvittaya, T., Duhl, T., Emmons, L. K., et al. (2012).

The model of emissions of gases and aerosols from nature version 2.1 (MEGAN2.1): An extended and updated framework for modeling biogenic emissions. *Geosci. Model Dev.* 5, 1471–1492. doi:10.5194/gmd-5-1471-2012.

Guenther, A., Zimmerman, P., Klinger, L., Greenberg, J., Ennis, C., Davis, K., et al. (1996). Estimates of regional natural volatile organic compound fluxes from enclosure and ambient measurements. *J. Geophys. Res. Atmos.* 101, 1345–1359. doi:10.1029/95JD03006.

Monson, R. K., Winkler, B., Rosenstiel, T. N., Block, K., Merl-Pham, J., Strauss, S. H., et al. (2020). High productivity in hybrid-poplar plantations without isoprene emission to the atmosphere. *Proc. Natl. Acad. Sci.* 117, 1596–1605. doi:10.1073/pnas.1912327117.

Nguyen, T. B., Crounse, J. D., Teng, A. P., St. Clair, J. M., Paulot, F., Wolfe, G. M., et al. (2015). Rapid deposition of oxidized biogenic compounds to a temperate forest. *Proc. Natl. Acad. Sci.* 112, E392–E401. doi:10.1073/pnas.1418702112.

Sharkey, T. D., Wiberley, A. E., and Donohue, A. R. (2008). Isoprene emission from plants: Why and how. *Ann. Bot.* 101, 5–18. doi:10.1093/aob/mcm240.

Španěl, P., Doren, J. M. V., and Smith, D. (2002). A selected ion flow tube study of the reactions of H3O+, NO+, and O2+ with saturated and unsaturated aldehydes and subsequent hydration of the product ions. *Int. J. Mass Spectrom.* 213, 163–176. doi:10.1016/S1387-3806(01)00531-0.

Vanzo, E., Jud, W., Li, Z., Albert, A., Domagalska, M. A., Ghirardo, A., et al. (2015). Facing the Future: Effects of Short-Term Climate Extremes on Isoprene-Emitting and Nonemitting Poplar. *Plant Physiol.* 169, 560–575. doi:10.1104/pp.15.00871.

Worton, D. R., Surratt, J. D., LaFranchi, B. W., Chan, A. W. H., Zhao, Y., Weber, R. J., et al. (2013). Observational Insights into Aerosol Formation from Isoprene. *Environ. Sci. Technol.* 47, 11403–11413. doi:10.1021/es4011064.

21st Aug 20

Dear Professor Hansel,

Your manuscript titled "Rapid Conversion of Isoprene Photooxidation Products in Terrestrial Plants " has now been seen by our reviewers, whose comments appear below. In light of their advice I am delighted to say that we are happy, in principle, to publish a suitably revised version in Communications Earth & Environment under the open access CC BY license (Creative Commons Attribution v4.0 International License).

We therefore invite you to revise your paper one last time to address the remaining concerns of our reviewers. At the same time we ask that you edit your manuscript to comply with our format requirements and to maximise the accessibility and therefore the impact of your work.

EDITORIAL REQUESTS:

Please review our specific editorial comments and requests regarding your manuscript in the attached "CommsEarth Final revisions information checklist". Please outline your response to each request in the right hand column.

SUBMISSION INFORMATION:

In order to accept your paper, we require the files outlined in the attached "CommsEarth Final submission file checklist.pdf"

OPEN ACCESS:

Communications Earth & Environment is a fully open access journal. Articles are made freely accessible on publication under a CC BY license (Creative Commons Attribution 4.0 International License). This license allows maximum dissemination and re-use of open access materials and is preferred by many research funding bodies.

For further information about article processing charges, open access funding, and advice and support from Nature Research, please visit https://www.nature.com/commsenv/about/open-access

At acceptance, the corresponding author will be required to complete an Open Access Licence to Publish on behalf of all authors, declare that all required third party permissions have been obtained and provide billing information in order to pay the article-processing charge (APC) via credit card or invoice.

Please note that your paper cannot be sent for typesetting to our production team until we have received these pieces of information; therefore, please ensure that you have this information ready when submitting the final version of your manuscript.

Please use the following link to submit the above items:
[link redacted]
** This url links to your confidential home page and associated information about manuscripts you may have submitted or be reviewing for us. If you wish to forward this email to co-authors, please delete the link to your homepage first **

We hope to hear from you within two weeks; please let us know if you need more time.

Best regards,

Heike Langenberg, PhD

Chief Editor
Communications Earth and Environment

On Twitter: @CommsEarth

REVIEWERS' COMMENTS:

Reviewer #1 (Remarks to the Author):

The reviewed manuscript and the point-by-point answer to the reviewers are mostly satisfactory. Authors have indeed added supplementary figures and text that answer most reviewers questions and imprrove the manuscript substantially.

I only have a few more comments on the new figures as well as a suggestion to being more cautious on the conclusion that the ISOPOOH deposition occurs mainly in the apoplast.

Indeed, to me Figure S6 does demonstrate that ISOPOOH is only deposited in the apoplast as when stomata close, water vapour at the leaf surface decrease and hence the possibility of a conversion of ISOPOOH at the leaf surface when it is wet because of stomatal aperture can not be ruled out. Additionally , the work of Nguyen et al. (2014) rather show that ISOPOOH canopy resistance is close to zero, suggesting that this compound may react outside of the plant and not enter the stomata (see Figure 4 of their paper). I find their work very convincing on that point.
However, since it is very difficult to design an experiment to separate stomatal and cuticular deposition, I would just suggest being more cautious and mention in the conclusions and abstract of the manuscript that stomatal uptake is very likely, but that leaf surface conversion may also occur. Leaf apoplastic extraction may be also performed but are difficult (see e.g. https://doi.org/10.1104/pp.18.01076).

Figure S6: Could you show the water vapour mixing ratio on the figure to better show demonstrate that the stomata are closed?

Figure S9: this is a very useful figure to demonstrate the link between AOR activity and MVK and

strengthen the conclusions of the paper.

Regarding the worldwide evaluation, I agree with the authors that many studies on VOCs have used chamber measurements to extrapolate to the globe. However, as pointed out by the authors, some comparison with field measurements have shown agreement within a factor of 2. It is therefore essential to recall the uncertainties around the worldwide estimations in the conclusions. These uncertainties include those linked with the chamber measurements as well as AOR activity changes with temperature, and the fact mechanism itself is not fully demontrsated as the stomatal uptake is not clearly demonstrated as the main uptake route.

See also additional comments in the text.

Reviewer #2 (Remarks to the Author):

Please check the description below
Page 6 in supporting information
"and we and wo the mole fraction of water vapor entering respectively leaving the enclosure (9, 10):"
should be
"and we and wo the mole fraction of water vapor entering and leaving the enclosure, respectively (9, 10):"

Rapid conversion of isoprene photooxidation products in terrestrial plants

Authors: Eva Canaval[1], Dylan B. Millet[2], Ina Zimmer[3], Tetyana Nosenko[3], Elisabeth Georgii[4], Eva Maria Partoll[1], Lukas Fischer[1], Hariprasad D. Alwe[2], Werner Jud[3], Markku Kulmala[5], Thomas Karl[6], Jörg-Peter Schnitzler[3], Armin Hansel[1*]

Affiliations:

[1]Department of Ion Physics and Applied Physics, University of Innsbruck, Innsbruck, Austria.

[2]Departement of Soil, Water and Climate, University of Minnesota, 439 Borlaug Hall, St. Paul MN, USA

[3]Helmholtz Zentrum München, Institute of Biochemical Plant Pathology, Research Unit Environmental Simulation, Neuherberg, Germany.

[4]Helmholtz Zentrum München, Institute of Biochemical Plant Pathology, Neuherberg, Germany

[5]Institute for Atmospheric and Earth System Research (INAR) / Physics, University of Helsinki, Helsinki 00014, Finland.

[6]Institute of Atmospheric and Cryospheric Sciences, University of Innsbruck, Innsbruck, Austria.

*Correspondence to: armin.hansel@uibk.ac.at

Isoprene is the dominant non-methane hydrocarbon emitted from the biosphere into the atmosphere, where it is preferentially oxidized to isoprene-hydroxy-hydroperoxides (ISOPOOH) at low NO_x or to methyl vinyl ketone (MVK) and methacrolein (MACR) at high NO_x. Here we show that 1,2-ISOPOOH deposits rapidly into poplar leaves where it undergoes conversion first to cytotoxic MVK and then enzymatically through alkenal/one oxidoreductase (AOR) to less toxic methyl ethyl ketone (MEK~~), which is emitted into the atmosphere. We analyzed *in situ* alkenal/one oxidoreductase (AOR) activity in leaf extracts from poplar plants fumigated with either 1,2-ISOPOOH or MVK and found that this enzyme was constitutively present in all leaf samples.~~ This detoxification process has global significance because AOR enzymes are ubiquitously present in terrestrial plants. Global chemistry-transport model simulations imply a re-emission of MEK from vegetation of 6.1 Tg yr^{-1}, making this the single largest MEK source ~~and recycling 1.5 % of the original isoprene flux~~. Eddy covariance flux measurements of isoprene and MEK over different forest ecosystems confirm that these MEK emissions reach 1-2 % those of isoprene. Our results suggest that detoxification processes in plants provides one of the most important OVOC sources in the atmosphere.

INTRODUCTION

Biogenic volatile organic compounds (BVOC) are thought to account for 90% of the total VOC emission into the Earth's atmosphere (*1*). Isoprene (C_5H_8) is the dominant BVOC with an estimated annual flux of 350-800 Tg yr^{-1} (*2*). Despite this large flux (mainly from broadleaf tree species) the question of why plants emit isoprene is still not fully understood ~~unresolved~~ (*3*). Recent hypotheses suggest that isoprene acts as a signaling molecule that, by altering gene expressions, strengthens plant defense mechanisms against oxidative and thermal stress (*4*). Once in the atmosphere isoprene reacts rapidly with OH radicals, which account for 90% of its total sink (*5*). Under typical daytime conditions isoprene is thus converted to oxidized VOC (OVOCs) within 1-2 hours (*6*). OH preferentially adds to the terminal carbons of isoprene, forming allyl radicals that in collisions with oxygen react to form HO-$C_5H_8O_2$ (ISOPOO) radicals. Subsequent oxidative steps depend critically on the ambient abundance of NO_x (NO + NO_2). At elevated NO_x, ISOPOO predominantly reacts with NO to form methyl vinyl ketone (MVK, yield 30-45%), methacrolein (MACR, yield 20-30%), and isoprene hydroxy nitrate (IHN, yield 13%) plus formaldehyde (HCHO) as the major products (*7*). Under low NO_x conditions the main product of ISOPOO reacting with HO_2 is isoprene hydroxy hydroperoxide (ISOPOOH), with the 1,2-ISOPOOH isomer formed in highest yield (*5*). Recently, Nguyen et al. (*8*) applied the eddy covariance (EC) technique to quantify the rapid dry deposition of ISOPOOH and other oxidized BVOC to a temperate forest. They determined a daytime mean deposition velocity (v_d) for ISOPOOH + IEPOX of 2.5 cm s^{-1} (IEPOX is an isomeric photooxidation product of ISOPOOH + OH). ISOPOOH+IEPOX deposition velocities (v_d) were then compared with a resistance model described elsewhere (*9*, *10*) to evaluate whether ISOPOOH+IEPOX is primarily lost to the leaf surface or taken up by the plants through their stomata. The calculated Henry's

law constant for ISOPOOH+IEPOX suggests a very small residual resistance favoring efficient uptake to any liquid surfaces (*8*). However, the v_d for ISOPOOH+IEPOX measured by Nguyen et al. (*8*) was too close to both the upper limit for stomata-controlled resistance and the upper limit for deposition without surface resistance to determine which mechanism is dominant. Thus, while direct EC flux measurements quantify the deposition of chemical species to the canopy, the fate of species at the leaf level – and thus any associated ecological impact – cannot be evaluated in this way. In the present study, we combine uptake rates and deposition velocities for 1,2-ISOPOOH and MVK obtained in laboratory experiments on gray poplars (*Populus* x *canescens*) with field observations using the EC technique in natural forest settings. Furthermore, we quantify the gene expression and enzyme activity of the detoxifying NADPH-dependent enzyme alkenal/one oxidoreductase (AOR) in poplar leaves and demonstrate the worldwide dissemination of AOR genes across terrestrial plants. Finally, we apply chemistry-transport modeling to assess atmospheric implications of our findings (see Methods for details). This enables the first leaf-to-global scale description of biosphere-atmosphere exchange for major isoprene photooxidation products, as summarized in Fig. 1.

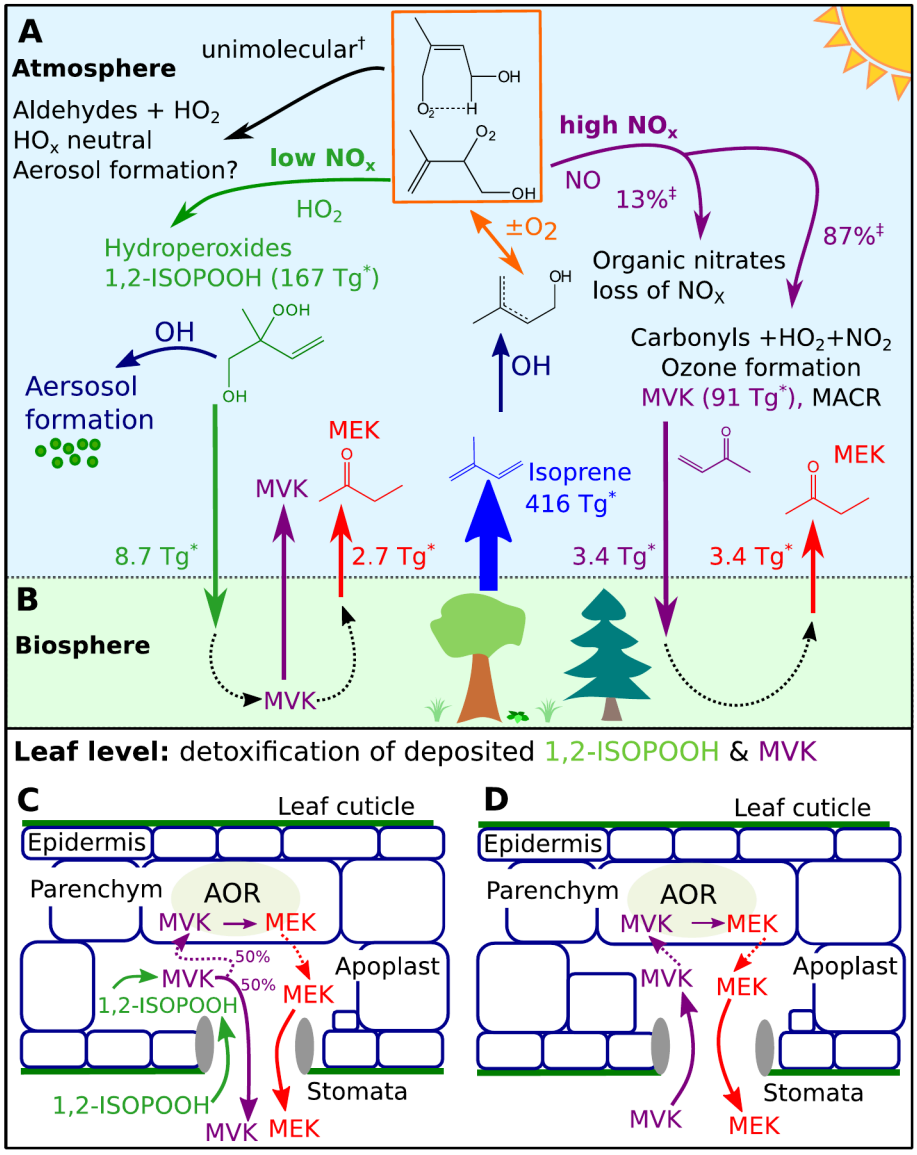

Fig. 1 Organic carbon exchange of major isoprene photooxidation products between the biosphere (B) and the atmosphere (A) on a global scale. Under low NO_x conditions 1,2-ISOPOOH is preferentially formed, producing epoxides that then react with OH and contribute to aerosol formation (*11*). At high NO_x the production of carbonyls such as MVK supports ozone formation (*5*). Dry-deposited 1,2-ISOPOOH and MVK is instantaneously detoxified within the plant leaf (C) via the enzyme alkenal/one oxidoreductase (AOR). EC measurements in natural forest settings confirm our modified GEOS-Chem model results (indicated with *) that approximately 6.1 Tg MEK (corresponding to 1.5% of the isoprene source) is emitted into the

atmosphere in this way. This is the single largest known MEK source on a global scale. † Values from ref. (*12*). ‡ Values from ref. (*7*).

RESULTS

Enclosure experiments

In a laboratory study, we investigated the fate of isoprene oxidation products when exposed to poplar leaves (Fig. 2, Supplementary Figure 1-4). Poplars occur worldwide, both in natural forests and plantations, and are among the most important boreal deciduous tree species. In plant science, poplars represent the most important model system for tree research and were the first tree species for which the genome was described. Many studies, in particular for VOCs, show that the biological and physiological processes studied in poplars can be transferred to other tree species (e.g. (*3*, *13*)). Poplar plants several months in age were selected for the present work because they allow gas exchange analyses and deposition experiments to be carried out in a very well-controlled and reproducible manner. Many VOC emission studies have shown that such results can be transferred to older trees and can hence be used for modelling studies on regional and global scales (e.g. (*2*, *14*)).

The experimental setup is illustrated in Supplementary Figure 1. Gray poplar plants were placed in an enclosure system and fumigated with synthetic air containing ~450 ppm CO_2 and ~8 ppbv 1,2-ISOPOOH. Before starting the plant fumigation experiments, we fumigated the empty cuvette with 1,2-ISOPOOH to condition the inner surfaces consisting of Teflon coated glass. Subsequently, the 1,2-ISOPOOH loss to the surface of the empty enclosure was measured for each individual experiment. The OVOC composition of the inlet and outlet air of the plant enclosure was analyzed with a selective reagent ion time-of- flight mass spectrometer (SRI-TOF-

MS). Details of the measurement method, SRI-TOF-MS instrument calibration, and plant material can be found in Methods ~~and SI Methods~~.

The deposition velocity $v_{d,i}$ (cm s^{-1}) is commonly used to describe trace gas deposition of a substance i to vegetation from the atmosphere (*15*) and is defined as the ratio between the flux Φ_i (representing the amount of compound i deposited to a unit surface area per unit time in µg cm^{-2} s^{-1}) and the local concentration c_i (µg cm^{-3}).

$$v_{d,i} = -\Phi_i / c_i \quad (1)$$

Deposition fluxes Φ_i to the plant surfaces inside the enclosure system were calculated from the difference in trace gas mixing ratios between the outlet of the enclosure ($c_{out,i}$) and outlet of the empty enclosure ($c_{out,i,BG}$) taking into account the single-sided leaf area (LA) of the enclosed plant and the gas flow (see SI). In this way, we calculated an average 1,2-ISOPOOH deposition velocity of v_d = 0.12 ± 0.04 cm s^{-1} under dark conditions (Fig. 2). The observed daytime value with open stomata (Supplementary Figure 5) is 0.79 ± 0.25 cm s^{-1}, close to the 24-h average simulated v_d of 0.76 cm s^{-1} from Nguyen et al. (*8*). Almost all deposited 1,2-ISOPOOH thus enters through open stomata into the plant's inner space, where it will dissolve on wetted surfaces due to its large effective solubility (H^* = 1.7x10^6 M atm^{-1}). Supplementary Figure 6 shows an experiment with a poplar plant exposed to elevated 1,2-ISOPOOH in the presence of light. Stomatal closure is observed, likely due to stress. Upon stomatal closure, 1,2-ISOPOOH levels in the enclosure increase, indicating that stomatal uptake is the dominant and not light-induced plant surface uptake. We further determine from these experiments that 50±15% of ~~stomatal~~ deposited 1,2-ISOPOOH is released as the volatile carbonyl MVK (H^* = 44 M atm^{-1})

while the other 50% is converted to MEK ($H^* = 21$ M atm^{-1}), which is likewise released back into the atmosphere.

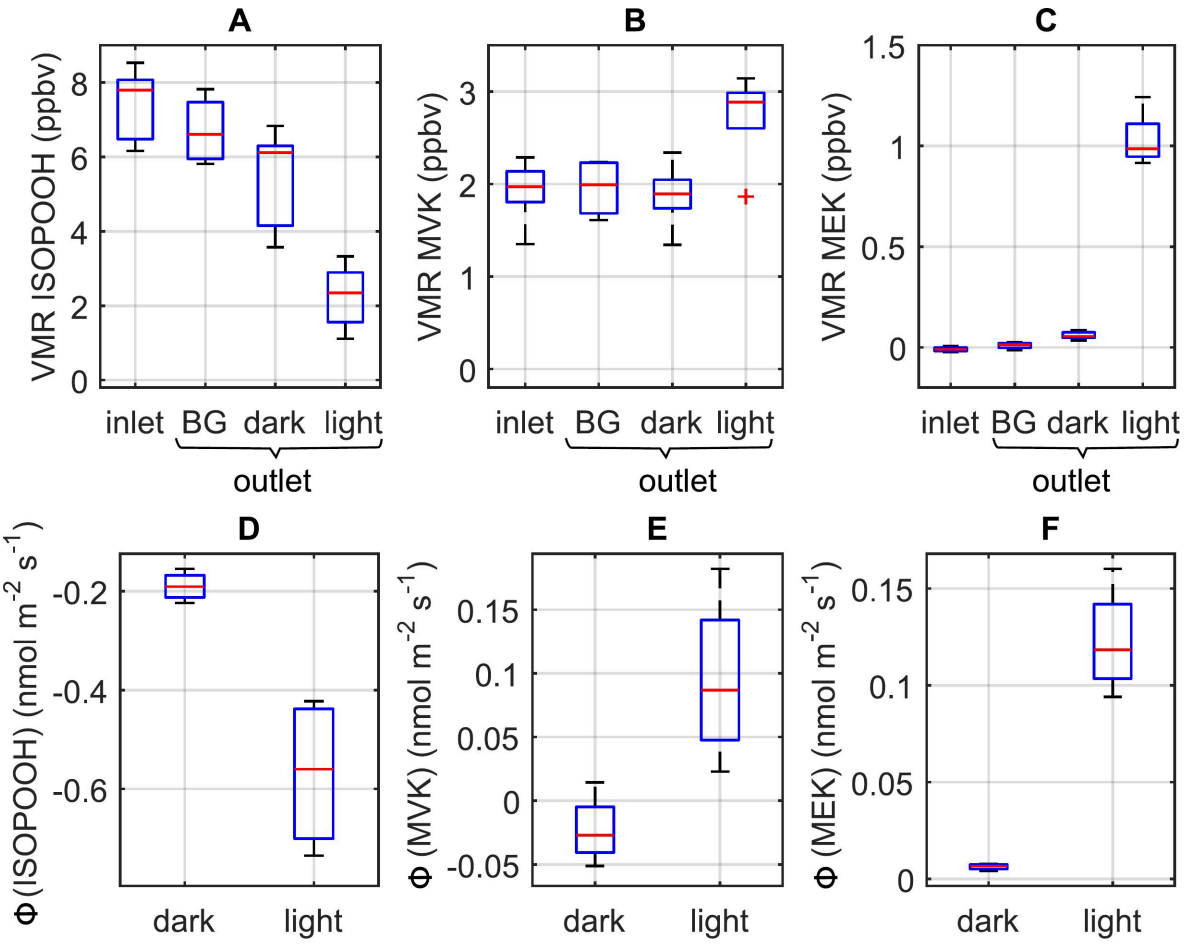

Fig. 2: Box plots of volume mixing ratios (VMR) (A-C) and deposition/emission fluxes (Φ) (D-F) for 1,2-ISOPOOH, MVK and MEK, respectively. OVOCs were analyzed at the enclosure inlet and subsequently at the enclosure outlet during fumigation of the empty enclosure (BG) and of the darkened/illuminated gray poplar trees. For each box, the red line indicates the median, bars show the minimum/maximum, and the blue box indicates the 25th and 75th percentiles of the sample data (N=5).

Organic hydroperoxides are inherently unstable species. Homolytic cleavage of the weak peroxy bond (O-OH) is a common decomposition mechanism, and can be catalyzed by metals (*16*). Recently, we have shown that 1,2-ISOPOOH is efficiently converted to MVK and HCHO on clean stainless steel surfaces (*17*, *18*). We find here from separate laboratory experiments (Supplementary Figure 7) that a range of different metals catalyze the conversion of 1,2-ISOPOOH to MVK even at room temperature. Chevallier et al. 2004 (*19*) studied "Fenton-like" reactions of methylhydroperoxides with Fe^{2+} in aqueous solutions. They identified Fe^{2+} + ROOH $\rightarrow$ Fe^{3+} + RO + OH as the dominant first reaction step. The alkoxy (RO) radicals further rearrange in water solution, and react with dissolved oxygen to form peroxy radicals which decompose, leading to the formation of aldehydes and other products. Assuming that the same reaction mechanism occurs when ISOPOOH dissolves in the liquid phase of the apoplast, low-valence transition metals present in plant cell walls and also dissolved in the apoplast (*20*) could catalyze via Fenton-type reactions the conversion of 1,2-ISOPOOH to MVK + HCHO + HO_2 in plant leaves. Since MVK (in contrast to formaldehyde) has relatively low solubility, it would then be released into the atmosphere through open stomata as its concentration builds up in the liquid phase of the apoplast. In biological systems peroxide functional groups (ROOH) serve as reactive oxygen intermediates that cause oxidative damage and cell death (*21*). For example, Polle and Junkermann (*22*) found hydroxymethyl hydroperoxide (HMHP) to inhibit peroxidase activity in plant apoplast. Plants exposed to harmful compounds in this way typically release stress-induced volatiles such as methyl salicylate (MeSA). MeSA is an airborne cue inducing pathogen resistance within and between plants (*23*), while also enhancing indirect plant defenses against herbivores by attracting their natural enemies (*24*). Furthermore, unstressed poplar varieties in general are weak sesquiterpene (SQT) emitters (*25*), but SQT emissions are known to

increase under various type of abiotic and biotic stresses (*26*, *27*). Here we observe a significant increase in emissions of both MeSA and SQT during 1,2-ISOPOOH fumigation (Supplementary Figure 8), but only under daylight conditions when stomata are open. Our laboratory experiments therefore indicate that stomatal uptake of 1,2-ISOPOOH causes severe stress to poplar plants and triggers self-defense mechanisms to mitigate oxidative damage. The results also indicate that upon deposition to plants, 1,2-ISOPOOH is converted as a first step to MVK. The exact reaction mechanism of this first step is not known. However, we speculate that the Fenton-type reactions discussed above involving transition metals present in plant cell walls and dissolved in the apoplast (*20*) catalyze the conversion of 1,2-ISOPOOH to MVK. As an α,β-unsaturated carbonyl and reactive electrophilic species, MVK itself is toxic to plant tissue due to its high reactivity and ability to form Michael adducts with the thiol and amino groups of biomolecules (*28*)(*29*). Previous MVK and MACR deposition experiments using poplars, three different Quercus species and houseplants have found both compounds to be immediately lost upon entry through open stomata (*30–32*). Tani et al (*31*) observed that the uptake rate correlates strongly with the stomatal conductance. Further, Cappellin et al. (*33*)(*34*) found that red oak (a strong isoprene emitter) converts MVK to MEK. Here we find based on additional MVK fumigation experiments with gray poplar plants (Supplementary Figure 4) that upon stomatal opening MVK fumigation leads to a significant increase in stress-related MeSA and SQT emissions (Supplementary Figure 8). Furthermore, the MVK detoxification mechanism is highly efficient: all (100±5%) deposited MVK is released as MEK into the atmosphere (Supplementary Figure 4). As shown by Tani et al. (*31*, *35*) and Cappellin et al. (*34*) MEK undergoes leaf uptake with significant lower rates than MVK. Average deposition velocities for MVK of v_d = 0.044 ± 0.045 cm s^{-1} and 0.22 ± 0.17 cm s^{-1} during dark and light conditions, respectively, are derived here, demonstrating the importance

of stomatal fluxes for this process. Poplar fumigation experiments with the 4,3-ISOPOOH isomer did not result in any MEK production. This finding is expected and supports the above proposed mechanism because 4,3-ISOPOOH is converted on metal surfaces to methacrolein (MACR) rather than MVK (*17*, *18*).

Enzymatic reactions within plant tissues

Several studies have shown that enzymatic reduction of α,β-unsaturated ketones takes place in plant suspension cells and cytosolic fractions of yeast (*36*, *37*). In particular, Yamauchi et al. (*38*) identified an NADPH-dependent acrolein-reducing enzyme in cucumber leaves that catalyzes an alkenal/one oxidoreductase (AOR) reaction of the α,β-unsaturated bond. We characterized the *in vitro* kinetic properties of the poplar AOR (EC 1.3.1.74) enzyme to which we attribute the in planta conversion of MVK to MEK. We obtain Michaelis-Menten constants (substrate concentration at half-maximal enzyme velocity) of 0.049 mM and 14.15 mM for NADPH and MVK, respectively, and a temperature optimum at 35°C (Supplementary Figure 9). ~~We find in our experiments a constitutively present *in vitro* AOR (EC 1.3.1.74) activity in leaf extracts, to which we attribute the *in planta* conversion of MVK to MEK.~~ This biochemical capability to reduce MVK to MEK is globally present in terrestrial plants, as a phylogenetic survey of genes coding for NADPH-dependent alkenal/on-oxidoreductases (AOR) demonstrates (Fig. 3, Supplementary Figure 10). One gene encoding AOR is localized in the chloroplast (AORchl), and two more are located in the cytosol (AORcyt-I and AORcyt-II; Fig. 3B and Supplementary Figure 10). The distribution of AORchl and AORcyt in plants is independent of isoprene and monoterpene emissions (Fig. 3A): AOR genes are ubiquitous in all land plants including mosses, clubmosses, gymnosperm and flowering plants (Supplementary Figure 10). Our gene expression analyses for gray poplar show that AORchl is predominantly expressed in leaf tissue, while

AORcyt-II is expressed in the stem (phloem and xylem) (Figure 3B). Under normal environmental conditions (*39*) the total gene expression rates of AORchl are more than six times those of AORcyt-II. We analyzed *in situ* AOR activity in leaf extracts from poplar plants fumigated with either 1,2-ISOPOOH or MVK (Supplementary Figure 11). The fact that we do not see any change to the *in situ* AOR activity as a result of exposure to 1,2-ISOPOOH and MVK (Supplementary Figure 11) may be due to the fact that our observation period was too short and missed a stress-induced response. However, AOR also belongs to a group of proteins that are post-translationally modified (PTM) by S-nitrosylation at certain cysteine residues under stress (Supplementary Figure 12, (*40*)), which may change in vitro enzyme activity. *In planta*, i.e. the intact leaves as we used for the gas exchange analyses, the AOR activity is variable depending on actual leaf temperature, light energy providing electrons in the form of NADPH for the reduction of MVK to MEK, and the presence of MVK, which is provided by deposition or degradation of 1,2-ISOPOOH. ~~AOR activity was present in all leaf samples (and unchanged during the short period of exposure to 1,2-ISOPOOH or MVK).~~ Overall, the phylogenetic analysis and the measurements of AOR activity in our model tree system imply that green biomass across the globe is able to convert MVK to MEK.

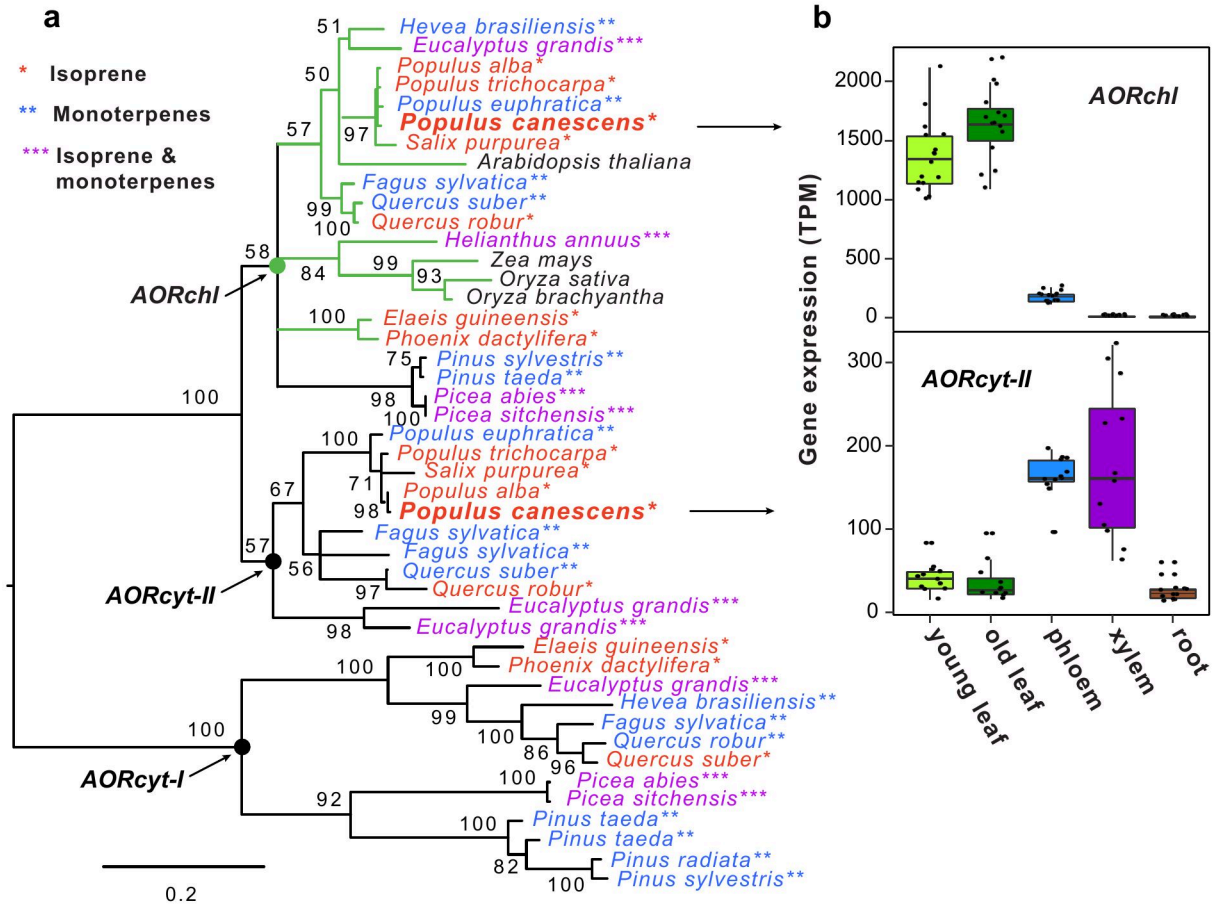

Fig. 3: Distribution of genes encoding AOR proteins. The Maximum likelihood (ML) phylogenetic tree (A) shows the occurrence of *AORchl*, *AORcyt-I* and *AORcyt-II* genes in dominant plant species. Asterisks and coloring of the branch labels indicate species emitting predominantly isoprene, monoterpenes, or both. Numbers at tree branches indicate node bootstrap support. Green branch coloring indicates the presence of plastid-targeting peptides (TP) in the corresponding AOR sequences. Basal nodes of the *AORchl*, *AORcyt-I* and *AORcyt-II* ortholog clusters are labeled with solid circles. The scale bar below the tree shows branch length. Box plots (B) show tissue-specific expression of *AORchl* and *AORcyt-II* genes in gray poplar (*Populus* x *canescens*).

Impact on regional and global budgets of OVOCs

We performed global simulations using the GEOS-Chem chemical transport model (CTM) (v12.1.1, doi:10.5281/zenodo.2249246) to assess how dry deposition of 1,2-ISOPOOH and

MVK (as the main isoprene oxidation products) impact the atmospheric MEK budget (see Methods and SI for model details). A global emission of 416 Tg isoprene is simulated by the model for 2017, leading to the photochemical production of 91.3 Tg MVK and 167 Tg 1,2-ISOPOOH (Fig. 4). By default, GEOS-Chem uses a modified resistance-based approach from Wesely (*9*) to calculate dry deposition velocities. The performance of this approach depends on knowledge about atmospheric stability, surface conditions, and the solubility and reactivity factors f_0 for compounds of interest. The stomatal fraction of 1,2-ISOPOOH dry deposition thus simulated by the model generally ranges from <5% to 30% over land (Supplementary Figure 13), which does not agree with our findings here (v_d = 0.78 cm s^{-1} during daytime versus only 0.10 cm s^{-1} in the dark). We therefore question how accurately the default model scheme is able to separate stomatal versus non-stomatal deposition for OVOCs. Instead, we prescribe the modeled 1,2-ISOPOOH and MVK deposition velocities over land based on the results from our laboratory measurements employing constant daytime (nighttime) deposition velocities of 0.22 (0.014) cm s^{-1} for MVK and 0.79 (0.12) cm s^{-1} for 1,2-ISOPOOH. Over oceans the default model scheme is used. Since the laboratory chambers were well-mixed, this corresponds to an assumption that canopy uptake for these compounds is controlled by surface and molecular diffusion ~~(rather than aerodynamic)~~ resistance, an assumption strongly supported by prior work (*8*). Figure 4 shows the resulting simulated global deposition of MVK (3.4 Tg) and 1,2-ISOPOOH (8.7 Tg). Assuming based on our measurements that 100% of dry deposited MVK and 50% of dry deposited 1,2-ISOPOOH undergoes conversion to MEK, the model yields a global MEK flux of 6.1 Tg (1.5% of isoprene emissions, Supplementary Figure 14), making this mechanism the largest known MEK source to the atmosphere (*41*). In turn, a fraction of that MEK will return to the ecosystem via further dry deposition (e.g., (*31*, *34*, *35*)).

For comparison, we performed a GEOS-Chem base-case run (Supplementary Figure 15) in which the default Wesely scheme was used to simulate 1,2-ISOPOOH and MVK dry deposition. Assuming that only the stomatal component of deposition leads to MEK then yields a global source of 3 Tg. We view this as a lower limit given the apparent underestimate of OVOC stomatal uptake in the default model. On the other hand, assuming that all dry deposited MVK and 50% of all dry deposited 1,2-ISOPOOH undergoes conversion results in an MEK source of 14 Tg (upper limit).

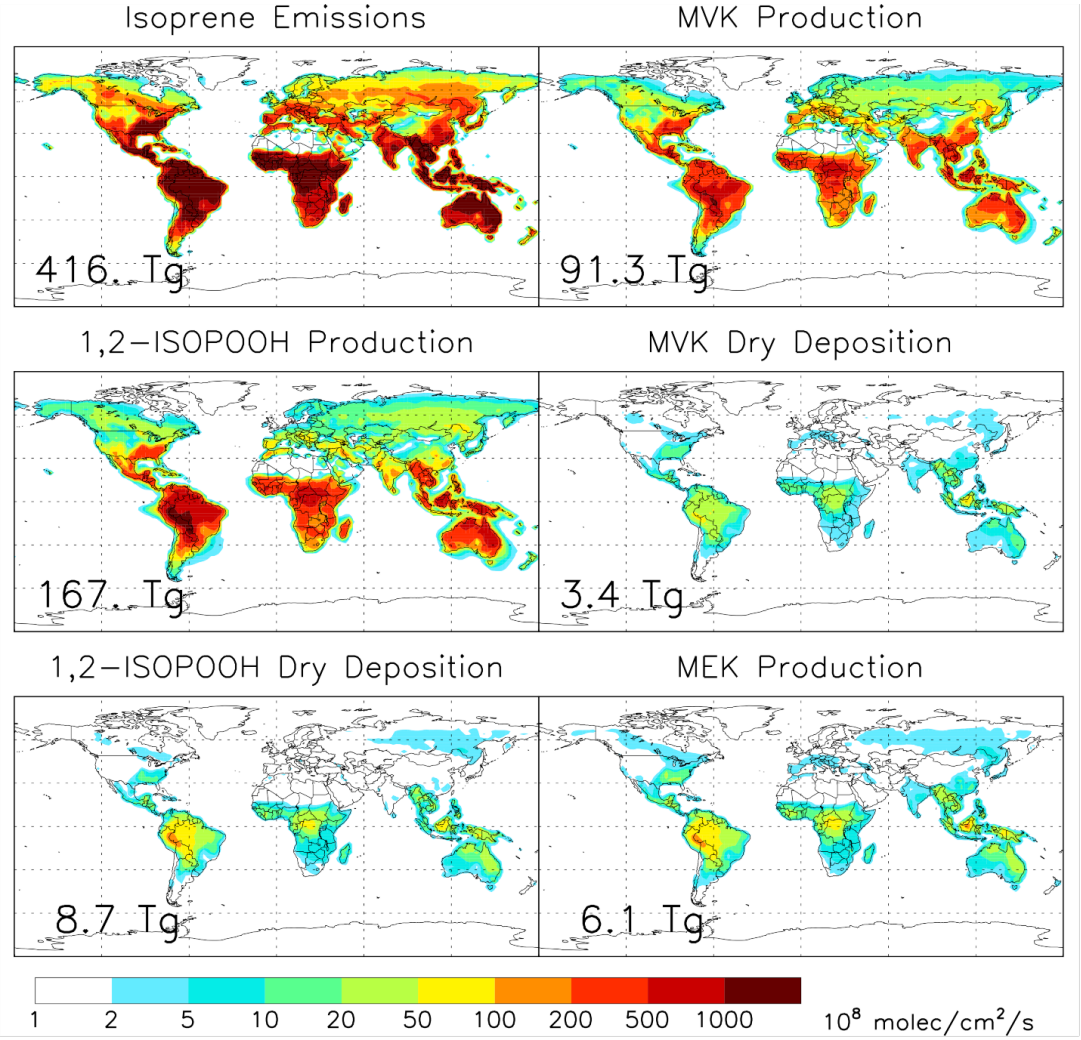

Fig. 4. Global isoprene emissions along with the production and deposition of key oxidation products (1,2-ISOPOOH, MVK) as simulated by the GEOS-Chem CTM for 2017 (see SI for model details). Reconciling the model deposition velocities using our experimentally-obtained $\boldsymbol{v_d}$, and assuming that 100% of dry deposited MVK and 50% of dry deposited 1,2-ISOPOOH undergoes conversion in plants, reveals a global MEK source of 6.1 Tg (and recycling 1.5% of the isoprene flux).

Eddy covariant VOC flux measurements

To evaluate these findings, we performed eddy covariant (EC) flux measurements of isoprene and MEK at two sites. The first is the SMEAR II station in Hyytiälä (Finland) (Supplementary Figure 16), which is surrounded by low isoprene-emitting plants (mainly Scots pine *Pinus*

279 *sylvestris*) with an average daytime isoprene flux of 1 nmol m^2 s^{-1} in spring. Details of the eddy
280 covariant VOC flux measurements can be found in Methods and SI. The second EC flux
281 measurements were performed at PROPHET (US) (Supplementary Figure 17), which is a high
282 isoprene emission site in a mixed deciduous/coniferous forest. Typical daytime isoprene flux
283 values at PROPHET reach ~10 nmol m^2 s^{-1} (Supplementary Figure 17). Flux data for isoprene
284 and MEK were obtained using the eddy covariance (EC) method, correlating fast mixing ratio
285 changes (~10 Hz) with vertical wind velocities. The high sensitivity achieved by the PTR3-TOF
286 for MEK (>12 000 cps/ppbv) enabled the first accurate measurement of these fluctuations at the
287 low isoprene-emission site. In general, the recent development of very sensitive, fast and
288 quantitative mass spectrometry-based detectors such as PTR-QiTOF and PTR3-TOF (*42*) was
289 essential for EC measurements of MEK. We find that MEK emissions are 1.8 % and 0.9 % those
290 of isoprene, at these sites respectively. This is in excellent agreement with the model best-
291 estimate (1.5%; see also Supplementary Figure 14) and supports the global importance of this
292 mechanism for plant oxidative protection and for the biogenic MEK atmospheric source.

293 **DISCUSSION**

294 Ketones are an important class of OVOC with sufficiently long atmospheric lifetimes to be
295 transported to the upper troposphere. MEK, like acetone, photolyzes in the near UV region; as a
296 result, these ketones provide an important source of HO_x (OH + HO_2) radicals in the dry upper
297 troposphere (*43*)(*44*). Degradation of MEK in the lower atmosphere generates toxic and photo-
298 active compounds such as acetaldehyde, a peroxyacetylnitrate (PAN) precursor, and
299 formaldehyde (*45*). Global sources of MEK, the second most abundant atmospheric ketone, are
300 still not fully understood. Singh et al. (*41*) presented a first assessment of MEK sources and sinks
301 based on aircraft measurements over the Pacific Ocean. Based on their derived MEK

atmospheric burden and an assumed 7-day lifetime due to reaction with OH and photolysis, they inferred a total global source of 11 Tg yr^{-1}. They further estimated MEK sources of 1-3 Tg yr^{-1} each from hydrocarbon oxidation and biomass burning, and of 0-1 Tg yr^{-1} from oceanic emissions. The latter estimate is supported by more recent analysis by Brewer et al. (*46*). A residual unexplained source of 7 Tg yr^{-1} was then attributed by Singh et al. (*41*) to direct biogenic emissions. Our work combining dedicated laboratory, field, and model analyses derives a global biogenic MEK source of 6.1 (3-14) Tg yr^{-1}, and provides a new biochemical and genetic basis for understanding the processes driving plant-atmosphere exchange of 1,2-ISOPOOH, MVK and MEK, and for modelling this exchange at regional and global scales.

~~Conclusion~~

Plants possess the ability to absorb OVOCs from the atmosphere and actively convert toxic chemicals to less toxic species, which can then be re-emitted into the atmosphere. Here we show that following ~~stomatal~~ uptake the toxic isoprene oxidation products 1,2-ISOPOOH and MVK are converted and re-emitted as MEK. The genes coding for the responsible enzyme alkenal/an oxidoreductase (AOR) are ubiquitously distributed in the plant kingdom. For MEK this process leads to an atmospheric input of about 6.1 Tg, the single largest known term in the global MEK budget and re-emitting 1.5% of the original isoprene emissions. Our findings thus support and provide a mechanistic underpinning to understand the biogenic emissions inferred by Singh et al. (*41*), and implicate detoxification as the most important source process in the global MEK budget. These findings suggest a significant modification of OVOCs at the biosphere-atmosphere interface. Traditional dry deposition schemes that are widely used in atmospheric chemistry models do not capture this process, and new mechanistic approaches should be developed to capture the complex behavior of bi-directional exchange at the biosphere-atmosphere interface.

METHODS

SRI-TOF-MS

The selective reagent ion time-of- flight mass spectrometer (SRI-TOF-MS) is a custom-built instrument that represents an advanced version of the PTR-TOF-MS system described by Graus et al. (*47*), and features the capability to switch between different reagent ions within seconds. Additionally, we replaced the standard metal drift rings of the reaction chamber with chemically inert conductive PEEK rings. This feature and the high flow rate through the reaction chamber (~800 ml min^{-1} instead of 10-30 ml min^{-1} in standard PTR-MS instruments) were essential for minimizing metal-catalyzed decomposition of 1,2-ISOPOOH as observed in standard PTR-MS instruments (*17*). The OVOC composition of the inlet and outlet air of the plant enclosure system was sequentially analyzed by SRI-TOF-MS operated with ammonia (NH_4^+) and occasionally with nitronium (NO^+) or hydronium (H_3O^+) reagent cations. The SRI-TOF-MS was operated at a constant temperature (35°C) and pressure (2.3 mbar) in the drift tube. Different drift voltages of 250, 300 and 500 V resulting in E/N values of 45 Td (NH_4^+-mode), 54 Td (NO^+-mode) and 90 Td (H_3O^+-mode), respectively, were used (E is the electric field strength, while N is the number gas density; 1Td = 10^{-17} Vcm^2). Raw data analysis was performed with the PTR-TOF-Data Analyzer (*48*) and the data processing routine described in Breitenlechner et al. (*42*). For details about chemical ionization mechanism and calibration of the SRI-TOF-MS see the Supplementary Information.

PTR3-TOF

The recently developed *PTR3-TOF* instrument (*42*) uses a discharge ion source coupled to a contact-free inlet system running at high sample gas flow rates through the novel reaction

chamber at 80 mbar. The PTR3 front portion is coupled to a TOF from TOFWERK mass analyzer. The instrument has sensitivities of up to 20 000 cps per ppbv and a mass resolution of approximately 8 000 m/Δm. VOCs were ionized via reactions with $H_3O^+(H_2O)_n$ primary ions. Flux data for isoprene and MEK were obtained using the eddy covariance (EC) method, correlating fast mixing ratio changes (~10 Hz) with vertical wind velocities. The high sensitivity achieved by the PTR3-TOF for MEK (>12 000 cps/ppbv) enables more accurate measurement of these fluctuations than was previously possible. Calibration details are described in the Supplementary Information.

Plant Material

In the present study we used 4-month old gray poplars (*Populus* x *canescens* INRA clone 7171-B4; syn. *P. tremula* x *P. alba* (Aiton.) Smith). Gray poplar shoots had been amplified by micropropagation on half-concentrated MS medium and further cultivated at the Helmholtz Zentrum München to an age of three months as described elsewhere (*49*). Before being used in the experiments, the poplar plants were grown in a greenhouse at the Institute of Microbiology of the University of Innsbruck for 1 to 4 weeks under natural light conditions. One day prior to the experiment, the plants were transferred to the laboratory to adapt to the light conditions (12-hour photoperiod with an approximate PAR of 400 µmol photons m^{-2} s^{-1}). All plants were well watered and showed no visible illness symptoms.

Determination AOR Activity

To determine apparent *in vitro* AOR activities in poplar leaf protein extracts, we deep-froze three mature leaves (leaf # 9-11, below the apex) from each poplar plant with liquid nitrogen at the

following experimental phases: (1) before the experiments, (2) immediately after the experiment, i.e., after 24 hours of ISOPOOH fumigation (12 hours illuminated and 12 hours in the dark), and (3) 24 hours after the end of the enclosure experiment. The apparent *in vitro* AOR (alkenal/one oxidoreductase) activity was assessed as described in Yamauchi et al. (*50*). Frozen leaf material was ground in liquid nitrogen using a dismembrator ball mill (B. Braun Biotech International, Melsungen, Germany). 200 mg of leaf powder were extracted in 4 ml of plant extraction buffer (100 mM Tris/HCl, pH 8.0, 20 mM $MgCl_2$, 100 mM $CaCl_2$, 1.5% PEG1500 (w/v), 5% (v/v) glycerol, 0.1% (v/v) Tween-20 and 20 mM DTT) with 200 mg polyvinylpolypyrrolidone (PVPP), stirred for 15 min on ice (4°C) and centrifuged for 15 min. at 20,000 *g*. The supernatant was purified on Sephadex G-25 PD-10 columns (GE Healthcare, Solingen, Germany) equilibrated with enzyme buffer (50 mM Tris/HCl, 20 mM $MgCl_2$, 5% (v/v) glycerol, 2 mM DTT) (*51*). Protein concentrations were determined by the Bradford assay using a Roti-Quant Kit (Carl Roth, Karlsruhe, Germany). Kinetic properties of AOR were initially characterized with changing concentrations of NADPH and MVK and at changing assay temperatures (Supplementary Figure 9). AOR activities were finally measured in crude protein extracts in the presence of 0.15 mM NADPH (under a saturating NADPH concentration; 3-times Michaelis-Menten constant (0.049 mM)), monitoring changes at A340 nm with a substrate concentration of 30 mM methyl vinyl ketone (MVK) (dissolved in enzyme buffer at a saturating MVK concentration of 2-times Michaelis-Menten constant (14.15 mM)) against a control without MVK according to (*50*) in a final assay volume of 1 mL. From extracts of 7 (1,2-ISOPOOH fumigation) and 5 (MVK fumigation) biological replicates three technical replicates were measured. A description of the construction of the AOR phylogenetic tree and AOR gene expression analysis can be found in the Supplementary Information.

EC flux Measurements

The first *EC flux measurement* site is situated at the SMEAR II station in Hyytiälä, Finland. Vegetation around the site is dominated by Scots pine (*Pinus sylvestris*) with a canopy height of approximately 15 m. The ground level vegetation consists of lingonberry (*Vaccinium vitis-idaea*), blueberry (*V. myrtillus*) and mosses (*Pleurozium scheberi, Dicramum polysetum*) (*52*). Flux data for isoprene and MEK were obtained with the PTR3 using the eddy covariance (EC) method during spring 2016. The PTR3 sampled air through a specially designed 5 m long tube with a high flow rate on top of a 35 m tower. Wind speed measurements were taken 0.5 m above the inlet opening by a METEK USA-1 sonic anemometer at 20 Hz. Wind direction and speed were cross checked against the SMEAR II station instrumentation.

The second EC flux measurement site is situated at the University of Michigan Biological Station (UMBS). Isoprene, MEK and other VOCs were measured by PTR-QiTOF as part of the PROPHET-AMOS field study in July 2016 (*53*, *54*). The 34 m PROPHET tower (45.559 °N, 84.715°W, 232 m elevation) is located in a mixed deciduous/coniferous forest (canopy height ~23 m) with an upper canopy dominated by aspen, birch and red oak and a lower canopy consisting mainly of white pine, red maple, beech, and red oak (*55*, *56*). Net above-canopy VOC fluxes were measured each hour by eddy covariance throughout the campaign. Sampling, instrument operation, calibration procedures, data processing, and QA/QC are described in detail elsewhere (*53*).

GEOS-Chem Model

GEOS-Chem (v12.1.1, doi:10.5281/zenodo.2249246; www.geos-chem.org) is a global 3D CTM driven by assimilated meteorological fields (Goddard Earth Observation System Forward Processing product; GEOS-FP) from the NASA Global Modeling and Assimilation Office (GMAO). The GEOS-FP data have native horizontal resolution of 0.25° latitude x 0.3125° longitude with 72 vertical layers. For the year 2017 global simulations presented here, we degrade the horizontal resolution to 2° x 2.5° and use a 15-min transport time step. We use the TPCORE advection algorithm (*57*), convective mass fluxes from the GEOS-FP archive (*58*), and the non-local boundary layer mixing scheme described by Lin and McElroy (*59*).

~~Wet deposition proceeds as described by Amos et al. (*60*). The default dry deposition in GEOS-Chem employs the modified Wesely (1989) scheme (*9*) implemented by Wang et al. (*61*) with updated treatment for OVOCs based on recent field constraints (*8*, *30*, *62*, *63*). Relevant parameters include H^* values of 1.7×10^6 M/atm for 1,2-ISOPOOH and 44 M/atm for MVK. Reactivity (f_0) values for both species are set to 1.0.~~Wet deposition in GEOS-Chem is as described by Amos et al. (*60*), and includes convective scavenging as well as rainout and washout by large-scale precipitation. The default dry deposition in GEOS-Chem employs the resistance-in-series scheme formulated by Wesely (*9*) and subsequently updated and implemented by Wang et al. (*61*) . Deposition velocities are computed in the model as a function of aerodynamic, boundary layer and surface resistances, with the first two computed from relevant molecular and meteorological parameters as detailed previously (*61*). Surface resistances incorporate stomatal, cuticular, lower canopy and ground surface pathways, and are likewise derived according to local environmental conditions (*61*, *64*). Relevant parameters for 1,2-ISOPOOH and MVK include H^* values of 1.7×10^6 M/atm and 44 M/atm, respectively, and reactivity (f_0) values of 1.0 for both species.

The GEOS-Chem chemical mechanism (publicly available online via doi:10.5281/zenodo.2249246) includes comprehensive HO_x-NO_x-VOC-ozone-halogen chemistry coupled to aerosols and incorporates current JPL/IUPAC recommendations with recent updates for isoprene chemistry (*62*, *65*), peroxyacetyl nitrate (*66*) and Criegee chemistry (*67*). Photolysis frequencies are calculated for 18 wavelength bins spanning 177-850 nm using the Fast-JX algorithms developed by Bian and Prather (*68*, *69*). Biogenic VOC emissions are computed online based on the Model of Emissions of Gases and Aerosols from Nature (MEGANv2.1; (*2*)) as described by Hu et al. (*70*). Specifically, emissions for each model grid cell are computed from vegetation-specific emission factors and multiplicative non-dimensional activity factors accounting for emission dependencies on light, temperature, leaf area, and leaf age (*2*). Biogenic MEK fluxes are computed separately by applying our laboratory measured-yields (100% and 50%, respectively) to the modeled MVK and ISOPOOH deposition fluxes as detailed in the main text. Global anthropogenic emissions of VOCs, CO, NH_3, NO_x, SO_2 and aerosols are from the Community Emissions Data System (CEDS) inventory (*71*) overwritten by regionally specific inventories for North America (*72*), Asia (*73*) and Africa (*74*). Biogenic soil NO_x emissions are from Hudman et al. (*75*).

Data availability

The data that support the findings of this study are available from the corresponding author upon reasonable request.

Code availability

We performed global simulations using the GEOS-Chem chemical transport model (CTM) (v12.1.1, doi:10.5281/zenodo.2249246), which is freely available at www.geos-chem.org.

References

1. A. H. Goldstein, I. E. Galbally, Known and unexplored organic constituents in the Earth's atmosphere. *Environ. Sci. Technol.* **41**, 1514–1521 (2007).

2. A. B. Guenther, X. Jiang, C. L. Heald, T. Sakulyanontvittaya, T. Duhl, L. K. Emmons, X. Wang, The model of emissions of gases and aerosols from nature version 2.1 (MEGAN2.1): An extended and updated framework for modeling biogenic emissions. *Geosci. Model Dev.* **5**, 1471–1492 (2012).

3. T. D. Sharkey, A. E. Wiberley, A. R. Donohue, Isoprene emission from plants: Why and how. *Ann. Bot.* **101**, 5–18 (2008).

4. A. T. Lantz, J. Allman, S. M. Weraduwage, T. D. Sharkey, Isoprene: New insights into the control of emission and mediation of stress tolerance by gene expression. *Plant. Cell Environ.* **42**, 2808–2826 (2019).

5. P. O. Wennberg, K. H. Bates, J. D. Crounse, L. G. Dodson, R. C. McVay, L. A. Mertens, T. B. Nguyen, E. Praske, R. H. Schwantes, M. D. Smarte, J. M. St Clair, A. P. Teng, X. Zhang, J. H. Seinfeld, Gas-phase reactions of isoprene and its major oxidation products. *Chem. Rev.* **118**, 3337–3390 (2018).

6. R. Atkinson, J. Arey, Gas-phase tropospheric chemistry of biogenic volatile organic compounds: a review. *Atmos. Environ.* **37**, 197–219 (2003).

7. A. P. Teng, J. D. Crounse, P. O. Wennberg, Isoprene peroxy radical dynamics. *J. Am. Chem. Soc.* **139**, 5367–5377 (2017).

8. T. B. Nguyen, J. D. Crounse, A. P. Teng, J. M. St. Clair, F. Paulot, G. M. Wolfe, P. O. Wennberg, Rapid deposition of oxidized biogenic compounds to a temperate forest. *Proc. Natl. Acad. Sci.* **112**, E392–E401 (2015).

9. M. L. Wesely, Parameterization of surface resistances to gaseous dry deposition in regional-scale numerical models. *Atmos. Environ.* **23**, 1293–1304 (1989).

10. M. Wesely, A review of the current status of knowledge on dry deposition. *Atmos. Environ.* **34**, 2261–2282 (2000).

11. F. Paulot, J. D. Crounse, H. G. Kjaergaard, A. Kurten, J. M. St. Clair, J. H. Seinfeld, P. O. Wennberg, Unexpected epoxide formation in the gas-phase photooxidation of isoprene. *Science (80-.).* **325**, 730–733 (2009).

12. T. Berndt, N. Hyttinen, H. Herrmann, A. Hansel, First oxidation products from the reaction of hydroxyl radicals with isoprene for pristine environmental conditions. *Commun. Chem.* **2**, 21 (2019).

13. I. T. Baldwin, J. C. Schultz, Rapid Changes in Tree Leaf Chemistry Induced by Damage: Evidence for Communication Between Plants. *Science (80-.).* **221**, 277–279 (1983).

14. R. K. Monson, B. Winkler, T. N. Rosenstiel, K. Block, J. Merl-Pham, S. H. Strauss, K. Ault, J. Maxfield, D. J. P. Moore, N. A. Trahan, A. A. Neice, I. Shiach, G. A. Barron-Gafford, P. Ibsen, J. T. McCorkel, J. Bernhardt, J.-P. Schnitzler, High productivity in hybrid-poplar plantations without isoprene emission to the atmosphere. *Proc. Natl. Acad. Sci.* **117**, 1596–1605 (2020).

15. J. H. Seinfeld, S. N. Pandis, *Atmospheric chemistry and physics : from air pollution to climate change* (John Wiley & Sons, 2012).

16. H. J. H. Fenton, LXXIII.—Oxidation of tartaric acid in presence of iron. *J. Chem. Soc., Trans.* **65**, 899–910 (1894).

17. J. C. Rivera-Rios, T. B. Nguyen, J. D. Crounse, W. Jud, J. M. St. Clair, T. Mikoviny, J. B. Gilman, B. M. Lerner, J. B. Kaiser, J. de Gouw, A. Wisthaler, A. Hansel, P. O. Wennberg, J. H. Seinfeld, F. N. Keutsch, Conversion of hydroperoxides to carbonyls in field and laboratory instrumentation: Observational bias in diagnosing pristine versus anthropogenically controlled atmospheric chemistry. *Geophys. Res. Lett.* **41**, 8645–8651 (2014).

18. A. K. Bernhammer, M. Breitenlechner, F. N. Keutsch, A. Hansel, Technical note: Conversion of isoprene hydroxy hydroperoxides (ISOPOOHs) on metal environmental simulation chamber walls. *Atmos. Chem. Phys.* **17**, 4053–4062 (2017).

19. E. Chevallier, R. D. Jolibois, N. Meunier, P. Carlier, A. Monod, "Fenton-like" reactions of methylhydroperoxide and ethylhydroperoxide with Fe^{2+} in liquid aerosols under tropospheric conditions. *Atmos. Environ.* **38**, 921–933 (2004).

20. B. Sattelmacher, The apoplast and its significance for plant mineral nutrition. *New Phytol.* **149**, 167–192 (2001).

21. R. Mittler, Oxidative stress, antioxidants and stress tolerance. *Trends Plant Sci.* **7**, 405–410 (2002).

22. A. Polle, W. Junkermann, Inhibition of apoplastic and symplastic peroxidase activity from Norway Spruce by the photooxidant hydroxymethyl hydroperoxide. *Plant Physiol.* **104**,

617–621 (1994).

23. V. Shulaev, P. Silverman, I. Raskin, Airborne signalling by methyl salicylate in plant pathogen resistance. *Nature*. **385** (1997), pp. 718–721.

24. E. Rowen, M. Gutensohn, N. Dudareva, I. Kaplan, Carnivore attractant or plant elicitor? Multifunctional roles of methyl salicylate lures in tomato defense. *J. Chem. Ecol.* **43**, 573–585 (2017).

25. J. Kesselmeier, M. Staudt, Biogenic volatile organic compounds (VOC): An overview on emission , physiology and ecology. *J. Atmos. Chem.* **33**, 23–88 (1999).

26. J.-P. Schnitzler, S. Louis, K. Behnke, M. Loivamäki, Poplar volatiles - biosynthesis, regulation and (eco)physiology of isoprene and stress-induced isoprenoids. *Plant Biol.* **12**, 302–316 (2010).

27. A. Ghirardo, J. Xie, X. Zheng, Y. Wang, R. Grote, K. Block, J. Wildt, T. Mentel, A. Kiendler-Scharr, M. Hallquist, K. Butterbach-Bahl, J. P. Schnitzler, Urban stress-induced biogenic VOC emissions and SOA-forming potentials in Beijing. *Atmos. Chem. Phys.* **16**, 2901–2920 (2016).

28. E. Alméras, S. Stolz, S. Vollenweider, P. Reymond, L. Mene-Saffrane, E. E. Farmer, Reactive electrophile species activate defense gene expression in Arabidopsis. *Plant J.* **34**, 205–216 (2003).

29. H. Esterbauer, R. J. Schaur, H. Zollner, Chemistry and biochemistry of 4-hydroxynonenal, malonaldehyde and related aldehydes. *Free Radic. Biol. Med.* **11**, 81–128 (1991).

30. T. Karl, P. Harley, L. Emmons, B. Thornton, A. Guenther, C. Basu, A. Turnipseed, K. Jardine, Efficient atmospheric cleansing of oxidized organic trace gases by vegetation.

549 *Science (80-.).* **330**, 816–819 (2010).

550 31. A. Tani, S. Tobe, S. Shimizu, Uptake of Methacrolein and Methyl Vinyl Ketone by Tree
551 Saplings and Implications for Forest Atmosphere. *Environ. Sci. Technol.* **44**, 7096–7101
552 (2010).

553 32. A. Tani, C. N. Hewitt, Uptake of aldehydes and ketones at typical indoor concentrations
554 by houseplants. *Environ. Sci. Technol.* **43**, 8338–8343 (2009).

555 33. L. Cappellin, A. Algarra Alarcon, I. Herdlinger-Blatt, J. Sanchez, F. Biasioli, S. T. Martin,
556 F. Loreto, K. A. McKinney, Field observations of volatile organic compound (VOC)
557 exchange in red oaks. *Atmos. Chem. Phys.* **17**, 4189–4207 (2017).

558 34. L. Cappellin, F. Loreto, F. Biasioli, P. Pastore, K. McKinney, A mechanism for biogenic
559 production and emission of MEK from MVK decoupled from isoprene biosynthesis.
560 *Atmos. Chem. Phys.* **19**, 3125–3135 (2019).

561 35. A. Tani, S. Tobe, S. Shimizu, Leaf uptake of methyl ethyl ketone and croton aldehyde by
562 Castanopsis sieboldii and Viburnum odoratissimum saplings. *Atmos. Environ.* **70**, 300–
563 306 (2013).

564 36. P. Wanner, R. Tressl, Purification and characterization of two enone reductases from
565 Saccharomyces cerevisiae. *Eur. J. Biochem.* **255**, 271–278 (1998).

566 37. A. Kergomard, M. F. Renard, H. Veschambre, D. Courtois, V. Petiard, Reduction of α,β-
567 unsaturated ketones by plant suspension cultures. *Phytochemistry*. **27**, 407–409 (1988).

568 38. Y. Yamauchi, A. Hasegawa, M. Mizutani, Y. Sugimoto, Chloroplastic NADPH-dependent
569 alkenal/one oxidoreductase contributes to the detoxification of reactive carbonyls
570 produced under oxidative stress. *FEBS Lett.* **586**, 1208–1213 (2012).

39. E. Georgii, K. Kugler, M. Pfeifer, E. Vanzo, K. Block, M. A. Domagalska, W. Jud, H. AbdElgawad, H. Asard, R. Reinhardt, A. Hansel, M. Spannagl, A. R. Schäffner, K. Palme, K. F. X. Mayer, J.-P. Schnitzler, The systems architecture of molecular memory in poplar after abiotic stress. *Plant Cell*. **31**, 346–367 (2019).

40. E. Vanzo, W. Jud, Z. Li, A. Albert, M. A. Domagalska, A. Ghirardo, B. Niederbacher, J. Frenzel, G. T. S. Beemster, H. Asard, H. Rennenberg, T. D. Sharkey, A. Hansel, J.-P. Schnitzler, Facing the Future: Effects of Short-Term Climate Extremes on Isoprene-Emitting and Nonemitting Poplar. *Plant Physiol.* **169**, 560–575 (2015).

41. H. B. Singh, L. J. Salas, R. B. Chatfield, E. Czech, A. Fried, J. Walega, M. J. Evans, B. D. Field, D. J. Jacob, D. Blake, B. Heikes, R. Talbot, G. Sachse, J. H. Crawford, M. A. Avery, S. Sandholm, H. Fuelberg, Analysis of the atmospheric distribution, sources, and sinks of oxygenated volatile organic chemicals based on measurements over the Pacific during TRACE-P. *J. Geophys. Res. D Atmos.* **109** (2004), doi:10.1029/2003JD003883.

42. M. Breitenlechner, L. Fischer, M. Hainer, M. Heinritzi, J. Curtius, A. Hansel, PTR3: An instrument for studying the lifecycle of reactive organic carbon in the atmosphere. *Anal. Chem.* **89**, 5824–5831 (2017).

43. H. B. Singh, M. Kanakidou, P. J. Crutzen, D. J. Jacob, High concentrations and photochemical fate of oxygenated hydrocarbons in the global troposphere. *Nature*. **378**, 50–54 (1995).

44. J. F. Brewer, D. K. Papanastasiou, J. B. Burkholder, E. V. Fischer, Y. Ren, A. Mellouki, A. R. Ravishankara, Atmospheric photolysis of methyl ethyl, diethyl, and propyl ethyl ketones: temperature-dependent UV absorption cross sections. *J. Geophys. Res. Atmos.*

124, 5906–5918 (2019).

45. M. E. Jenkin, S. M. Saunders, M. J. Pilling, The tropospheric degradation of volatile organic compounds: a protocol for mechanism development. *Atmos. Environ.* **31**, 81–104 (1997).

46. J. F. Brewer, E. V. Fischer, R. Commane, S. C. Wofsy, B. Daube, E. C. Apel, A. J. Hills, R. S. Hornbrook, B. Barletta, S. Meinardi, D. R. Blake, E. A. Ray, A. R. Ravishankara, Evidence for an oceanic source of methyl ethyl ketone to the atmosphere. *Geophys. Res. Lett.* **591**, 5022–5024 (2020).

47. M. Graus, M. Müller, A. Hansel, High resolution PTR-TOF: quantification and formula confirmation of VOC in real time. *J. Am. Soc. Mass Spectrom.* **21**, 1037–44 (2010).

48. M. Müller, T. Mikoviny, W. Jud, B. D'Anna, A. Wisthaler, A new software tool for the analysis of high resolution PTR-TOF mass spectra. *Chemom. Intell. Lab. Syst.* **127**, 158–165 (2013).

49. E. Vanzo, J. Merl-Pham, V. Velikova, A. Ghirardo, C. Lindermayr, S. M. Hauck, J. Bernhardt, K. Riedel, J. Durner, J.-P. Schnitzler, Modulation of protein S -nitrosylation by isoprene emission in poplar. *Plant Physiol.* **170**, 1945–1961 (2016).

50. Y. Yamauchi, A. Hasegawa, A. Taninaka, M. Mizutani, Y. Sugimoto, NADPH-dependent reductases involved in the detoxification of reactive carbonyls in plants. *J. Biol. Chem.* **286**, 6999–7009 (2011).

51. J. P. Schnitzler, I. Zimmer, A. Bachl, M. Arend, J. Fromm, R. J. Fischbach, Biochemical properties of isoprene synthase in poplar (*Populus x canescens*). *Planta*. **222**, 777–786 (2005).

52. H. Ilvesniemi, R. Giesler, P. Van Hees, T. Magnussson, P. A. Melkerud, General description of the sampling techniques and the sites investigated in the Fennoscandinavian podzolization project. *Geoderma*. **94**, 109–123 (2000).

53. D. B. Millet, H. D. Alwe, X. Chen, M. J. Deventer, T. J. Griffis, R. Holzinger, S. B. Bertman, P. S. Rickly, P. S. Stevens, T. Léonardis, N. Locoge, S. Dusanter, G. S. Tyndall, S. L. Alvarez, M. H. Erickson, J. H. Flynn, Bidirectional ecosystem-atmosphere fluxes of volatile organic compounds across the mass spectrum: How many matter? *ACS Earth Sp. Chem.* **2**, 764–777 (2018).

54. H. D. Alwe, D. B. Millet, X. Chen, J. D. Raff, Z. C. Payne, K. Fledderman, Oxidation of volatile organic compounds as the major source of formic acid in a mixed forest canopy. *Geophys. Res. Lett.* **46**, 2940–2948 (2019).

55. A. M. Bryan, S. J. Cheng, K. Ashworth, A. B. Guenther, B. S. Hardiman, G. Bohrer, A. L. Steiner, Forest-atmosphere BVOC exchange in diverse and structurally complex canopies: 1-D modeling of a mid-successional forest in northern Michigan. *Atmos. Environ.* **120**, 217–226 (2015).

56. B. J. Palik, K. S. Pregitzer, A comparison of presettlement and present-day forests on two bigtooth aspen-dominated landscapes in Northern Lower Michigan. *Am. Midl. Nat.* **127**, 327 (1992).

57. S.-J. Lin, R. B. Rood, Multidimensional flux-form semi-Lagrangian transport schemes. *Mon. Weather Rev.* **124**, 2046–2070 (2002).

58. X. Wu, L. Deng, X. Song, G. J. Zhang, Coupling of convective momentum transport with convective heating in global climate simulations. *J. Atmos. Sci.* **64**, 1334–1349 (2007).

59. J.-T. Lin, M. B. McElroy, Impacts of boundary layer mixing on pollutant vertical profiles in the lower troposphere: Implications to satellite remote sensing. *Atmos. Environ.* **44**, 1726–1739 (2010).

60. H. M. Amos, D. J. Jacob, C. D. Holmes, J. A. Fisher, Q. Wang, R. M. Yantosca, E. S. Corbitt, E. Galarneau, A. P. Rutter, M. S. Gustin, A. Steffen, J. J. Schauer, J. A. Graydon, V. L. St Louis, R. W. Talbot, E. S. Edgerton, Y. Zhang, E. M. Sunderland, Gas-particle partitioning of atmospheric Hg(II) and its effect on global mercury deposition. *Atmos. Chem. Phys.* **12**, 591–603 (2012).

61. Y. Wang, J. A. Logan, D. J. Jacob, Global simulation of tropospheric O_3 -NO_x-hydrocarbon chemistry: 2. Model evaluation and global ozone budget. *J. Geophys. Res. Atmos.* **103**, 10727–10755 (1998).

62. K. R. Travis, D. J. Jacob, J. A. Fisher, P. S. Kim, E. A. Marais, L. Zhu, K. Yu, C. C. Miller, R. M. Yantosca, M. P. Sulprizio, A. M. Thompson, P. O. Wennberg, J. D. Crounse, J. M. St Clair, R. C. Cohen, J. L. Laughner, J. E. Dibb, S. R. Hall, K. Ullmann, G. M. Wolfe, I. B. Pollack, J. Peischl, J. A. Neuman, X. Zhou, Why do models overestimate surface ozone in the Southeast United States? *Atmos. Chem. Phys.* **16**, 13561–13577 (2016).

63. E. A. Marais, D. J. Jacob, J. L. Jimenez, P. Campuzano-Jost, D. A. Day, W. Hu, J. Krechmer, L. Zhu, P. S. Kim, C. C. Miller, J. A. Fisher, K. Travis, K. Yu, T. F. Hanisco, G. M. Wolfe, H. L. Arkinson, H. O. T. Pye, K. D. Froyd, J. Liao, V. F. McNeill, Aqueous-phase mechanism for secondary organic aerosol formation from isoprene: application to the southeast United States and co-benefit of SO_2 emission controls. *Atmos. Chem. Phys.* **16**, 1603–1618 (2016).

64. S. J. Silva, C. L. Heald, Investigating dry deposition of ozone to vegetation. *J. Geophys. Res. Atmos.* **123**, 559–573 (2018).

65. J. A. Fisher, D. J. Jacob, K. R. Travis, P. S. Kim, E. A. Marais, C. C. Miller, K. Yu, L. Zhu, R. M. Yantosca, M. P. Sulprizio, J. Mao, P. O. Wennberg, J. D. Crounse, A. P. Teng, T. B. Nguyen, J. M. S. Clair, R. C. Cohen, P. Romer, B. A. Nault, P. J. Wooldridge, J. L. Jimenez, P. Campuzano-Jost, D. A. Day, W. Hu, P. B. Shepson, F. Xiong, D. R. Blake, A. H. Goldstein, P. K. Misztal, T. F. Hanisco, G. M. Wolfe, T. B. Ryerson, A. Wisthaler, T. Mikoviny, Organic nitrate chemistry and its implications for nitrogen budgets in an isoprene- and monoterpene-rich atmosphere: Constraints from aircraft (SEAC 4 RS) and ground-based (SOAS) observations in the Southeast US. *Atmos. Chem. Phys.* **16**, 5969–5991 (2016).

66. E. V. Fischer, D. J. Jacob, R. M. Yantosca, M. P. Sulprizio, D. B. Millet, J. Mao, F. Paulot, H. B. Singh, A. Roiger, L. Ries, R. W. Talbot, K. Dzepina, S. Pandey Deolal, Atmospheric peroxyacetyl nitrate (PAN): a global budget and source attribution. *Atmos. Chem. Phys.* **14**, 2679–2698 (2014).

67. D. B. Millet, M. Baasandorj, D. K. Farmer, J. A. Thornton, K. Baumann, P. Brophy, S. Chaliyakunnel, J. A. De Gouw, M. Graus, L. Hu, A. Koss, B. H. Lee, F. D. Lopez-Hilfiker, J. A. Neuman, F. Paulot, J. Peischl, I. B. Pollack, T. B. Ryerson, C. Warneke, B. J. Williams, J. Xu, A large and ubiquitous source of atmospheric formic acid. *Atmos. Chem. Phys.* **15**, 6283–6304 (2015).

68. H. Bian, M. J. Prather, Fast-J2: Accurate simulation of stratospheric photolysis in global chemical models. *J. Atmos. Chem.* **41**, 281–296 (2002).

69. S. D. Eastham, D. K. Weisenstein, S. R. H. Barrett, Development and evaluation of the unified tropospheric-stratospheric chemistry extension (UCX) for the global chemistry-transport model GEOS-Chem. *Atmos. Environ.* **89**, 52–63 (2014).

70. L. Hu, D. B. Millet, M. Baasandorj, T. J. Griffis, P. Turner, D. Helmig, A. J. Curtis, J. Hueber, Isoprene emissions and impacts over an ecological transition region in the U.S. Upper Midwest inferred from tall tower measurements. *J. Geophys. Res.* **120**, 3553–3571 (2015).

71. R. M. Hoesly, S. J. Smith, L. Feng, Z. Klimont, G. Janssens-Maenhout, T. Pitkanen, J. J. Seibert, L. Vu, R. J. Andres, R. M. Bolt, T. C. Bond, L. Dawidowski, N. Kholod, J. Kurokawa, M. Li, L. Liu, Z. Lu, M. C. P. Moura, P. R. O&amp, apos, Rourke, Q. Zhang, Historical (1750–2014) anthropogenic emissions of reactive gases and aerosols from the Community Emissions Data System (CEDS). *Geosci. Model Dev.* **11**, 369–408 (2018).

72. EPA, 2011 National Emissions Inventory Data & Documentation (2015), (available at https://www.epa.gov/air-emissions-inventories/2011-national-emission-inventory-nei-report).

73. M. Li, Q. Zhang, J. I. Kurokawa, J. H. Woo, K. He, Z. Lu, T. Ohara, Y. Song, D. G. Streets, G. R. Carmichael, Y. Cheng, C. Hong, H. Huo, X. Jiang, S. Kang, F. Liu, H. Su, B. Zheng, MIX: A mosaic Asian anthropogenic emission inventory under the international collaboration framework of the MICS-Asia and HTAP. *Atmos. Chem. Phys.* **17**, 935–963 (2017).

74. E. A. Marais, C. Wiedinmyer, Air quality impact of Diffuse and Inefficient Combustion Emissions in Africa (DICE-Africa). *Environ. Sci. Technol.* **50**, 10739–10745 (2016).

75. R. C. Hudman, N. E. Moore, A. K. Mebust, R. V. Martin, A. R. Russell, L. C. Valin, R. C. Cohen, Steps towards a mechanistic model of global soil nitric oxide emissions: Implementation and space based-constraints. *Atmos. Chem. Phys.* **12**, 7779–7795 (2012).

Acknowledgement

The authors would like to thank Bernhard Mentler (UIBK) for developing the ISOPOOH and IEPOX measurement protocol using different reagent ions, Ulrich Junghans (Helmholtz) for growing the sample plants, Frank Keutsch & Jean Rivera-Rios (Harvard University) for providing the 1,2-ISOPOOH standard and Holger Kopacka (UIBK) for the NMR analysis of the samples. We thank Xin Chen (UMN) for assistance with the model simulations, along with Steven Bertman (WMU) and the entire PROPHET-AMOS team for their support and contributions to the field campaign. We thank Martin Breitenlechner (UIBK) for contributions to the Hyytiälä field campaign. We thank the Institute of Microbiology from the University of Innsbruck for sharing the greenhouse facility.

Funding

This study was supported by the Austrian Federal Ministry of Education, Science and Research within Sparkling Science (grant SPA 05/080 - AiR and grant SPA 06/222 - CHAMPIONS). VOC flux measurements at Hyytiälä were supported by the European Commission under Horizon 2020, (H2020-INFRAIA-2014-2015, grant 654109, ACTRIS). VOC measurements during PROPHET were supported by the US National Science Foundation (NSF grants AGS-1428257 and AGS- 1148951). GEOS- Chem model development and simulations were supported by the US National Aeronautics and Space Administration (NASA grant NNX14AP89G). Computing resources at UMN were provided by MSI (www.msi.umn.edu).

Author contributions

AH, EC and JPS designed the experiment. EC, EP performed the laboratory measurements and data analysis, LF assisted with data analysis. IZ and JPS measured AOR activities. TN, EG and JPS generated the AOR phylogenesis. DBM, HDA, and LF contributed with eddy flux data. DBM ran the GEOS-Chem model and analyzed the results. WJ and TK took part in data discussion and manuscript improvement. The manuscript was written through contributions of all authors. All authors have given approval to the final version of the manuscript.

Additional information

Supplementary information is available in the online version of the paper.

Competing interests

Authors declare no competing interests.

Point-by-point response to the reviewer comments:

Final Revision

We would like to thank both reviewers for thoroughly reviewing our manuscript and for their final comments that helped to improve the manuscript. Our responses to the reviewer comments are below.

Reviewer #1:

The reviewed manuscript and the point-by-point answer to the reviewers are mostly satisfactory. Authors have indeed added supplementary figures and text that answer most reviewer's questions and improve the manuscript substantially.

I only have a few more comments on the new figures as well as a suggestion to being more cautious on the conclusion that the ISOPOOH deposition occurs mainly in the apoplast.

Indeed, to me Figure S6 does demonstrate that ISOPOOH is only deposited in the apoplast as when stomata close, water vapour at the leaf surface decrease and hence the possibility of a conversion of ISOPOOH at the leaf surface when it is wet because of stomatal aperture cannot be ruled out. Additionally, the work of Nguyen et al. (2014) rather show that ISOPOOH canopy resistance is close to zero, suggesting that this compound may react outside of the plant and not enter the stomata (see Figure 4 of their paper). I find their work very convincing on that point. However, since it is very difficult to design an experiment to separate stomatal and cuticular deposition, I would just suggest being more cautious and mention in the conclusions and abstract of the manuscript that stomatal uptake is very likely, but that leaf surface conversion may also occur. Leaf apoplastic extraction may be also performed but are difficult (see e.g. https://doi.org/10.1104/pp.18.01076).

Response:

We agree with the reviewer's comment to be more cautious and mention in the conclusion and in the abstract that stomatal uptake is very likely, but that leaf surface conversion may also occur.

We have now used **your edited abstract** with following minor changes:

- We added "most probably" to soften our conclusion. The sentence reads now: There, it is converted first to cytotoxic MVK and then "most probably" through alkenal/one oxidoreductase (AOR) to less toxic methyl ethyl ketone (MEK).
- We changed 6.1 Tg yr^{-1} to 6.5 Tg yr^{-1} due to new results from GEOS-Chem simulations utilizing humidity corrected deposition velocities (reviewer #2 final comment of 1st revision).
- We added "presently known" and deleted "if correct". The sentence reads now: This is the single largest MEK source "presently known", and recycles 1.5 % of the original isoprene flux

In the results section (lines 166-167) we use now a more cautious wording:

- ..is most probably the dominant deposition process, and light-induced plant surface uptake is less likely.

Figure S6: Could you show the water vapour mixing ratio on the figure to better show demonstrate that the stomata are closed?

> ***Response:*** We now show the difference of the water vapour mixing ratio between inlet and outlet of the enclosure in Figure S6. The data indicate stomatal closing.

Figure S9: this is a very useful figure to demonstrate the link between AOR activity and MVK and strengthen the conclusions of the paper.

Regarding the worldwide evaluation, I agree with the authors that many studies on VOCs have used chamber measurements to extrapolate to the globe. However, as pointed out by the authors, some comparison with field measurements have shown agreement within a factor of 2. It is therefore essential to recall the uncertainties around the worldwide estimations in the conclusions. These uncertainties include those linked with the chamber measurements as well as AOR activity changes with temperature, and the fact mechanism itself is not fully demonstrated as the stomatal uptake is not clearly demonstrated as the main uptake route.

> ***Response:*** We added the following statement in the conclusion (lines 291 ff):
> "The global MEK estimate has uncertainties due to the underlying up-scaling errors. These uncertainties include those linked with the enclosure measurements as well as AOR activity changes with temperature. We found in enclosure measurements that stomatal uptake is the dominant route, but leaf surface conversion on wet surfaces may also occur under real world conditions. However, for many years scientists have used plant enclosure experiments in combination with field-based flux measurements to better asses global BVOC emissions. For example, Guenther et al. (45) compared BVOC flux estimates from enclosure and ambient measurements and found agreement to within a factor of two."

See also additional comments in the text.

> ***Response:*** We change the manuscript according to the comments in the text.

Reviewer #2 (Remarks to the Author):

Please check the description below
Page 6 in supporting information
"and we and wo the mole fraction of water vapor entering ***respectively*** leaving the enclosure (9, 10):"
should be
"and we and wo the mole fraction of water vapor entering and leaving the enclosure, ***respectively*** (9, 10):"

> ***Response:*** We changed the text accordingly.

Additional changes:

Reviewer #2 asked for humidity corrected deposition velocities in his final comment of the 1st revision, the values of which we provide in response to the 1st revision.
Meanwhile we performed also a new global GEOS-Chem simulation utilizing humidity corrected deposition velocities and found minor changes (see Figure below):

The global 1,2-ISOPOOH dry deposition changed from 8.7 to 8.8 Tg yr^{-1}.
The global MVK dry deposition changed from 3.4 to 3.7 Tg yr^{-1}.
The global MEK production changed from 6.1 to 6.5 Tg yr^{-1}.

In the final manuscript and final supplementary information, we used the new values and updated corresponding Figures (Figure 4 and Supplementary Figure 14).

Fig 4 (2x2.5 degrees, old simulation)

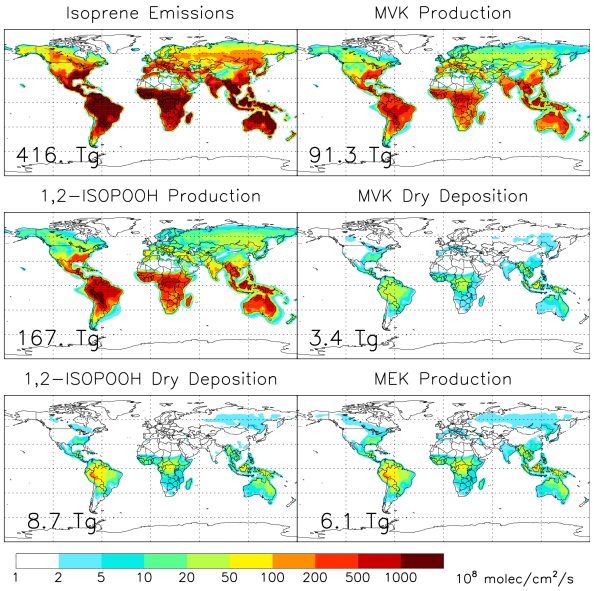

Fig 4 (2x2.5 degrees, new simulation)

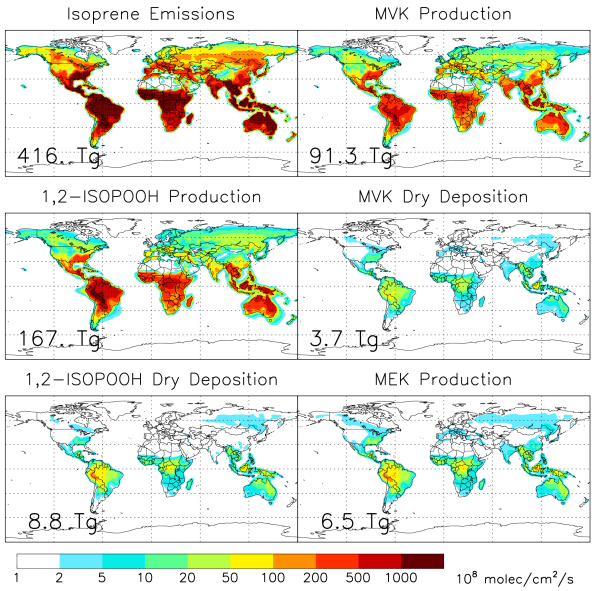

Guenther, A., Zimmerman, P., Klinger, L., Greenberg, J., Ennis, C., Davis, K., et al. (1996). Estimates of regional natural volatile organic compound fluxes from enclosure and ambient measurements. *J. Geophys. Res. Atmos.* 101, 1345–1359. doi:10.1029/95JD03006.